Predicting population viability of the narrow endemic Mediterranean plant Centaurea corymbosa under climate change

Asma Hadjou Belaid, Sandrine Maurice, Hélène Freville, David Carbonell, Eric Imbert

Title:

Predicting population viability of the narrow endemic Mediterranean plant *Centaurea corymbosa* under climate change.

Authors:

Asma HADJOU BELAID[a], Sandrine MAURICE[a], Hélène FREVILLE[b], David CARBONELL[a], Eric IMBERT[a,*]

Address:

[a] ISEM-Université de Montpellier, CNRS, IRD, EPHE-Montpellier, France.

[b] AGAP,Univ Montpellier, CIRAD, INRA, Montpellier SupAgro - Montpellier, France

[*] **Corresponding author:** Eric IMBERT, eric.imbert@umontpellier.fr

Title:

Predicting population viability of the narrow endemic Mediterranean plant *Centaurea corymbosa* under climate change.

Abstract

Climate change is a growing threat for global biodiversity, in particular for narrow endemic species. The Mediterranean region, which harbors an exceptional biodiversity, has been identified as one of the most sensitive regions to climate change. Based on a 22-year monitoring period, we analyzed the dynamic and viability of the six extant populations of a narrow endemic plant species of the Mediterranean area, *Centaurea corymbosa*, to predict their fate under two climatic scenarios. We constructed matrix projection models to calculate current asymptotic growth rates and to perform stochastic projections including both demographic and environmental stochasticity. Neither asymptotic growth rates nor their temporal variance were linked to population size and age at flowering. Randomization tests showed that asymptotic growth rates were significantly different among years but not among populations. An increase in temperature and a decrease in the number of wet days had a negative impact on the whole life-cycle, particularly in the summer period, and thus reduced asymptotic growth rates. Stochastic projections showed that an increased frequency of extreme climatic events increased population extinction risk and decreased mean time to extinction. The warm scenario had a more dramatic impact on population viability than the dry scenario. Management recommendations are proposed to increase population viability of endangered plant species such as *C. corymbosa* that face climate change.

1

1. Introduction

Ongoing climate change is expected to result in increase in drought and warm periods in several regions due to both an increasing frequency of extreme climatic events and long-term gradual changes (IPCC, 2007). Compared to some other taxonomic groups, plants are more vulnerable to climate change since they have relatively low migration capacity (Malcolm et al., 2006; Thomas et al., 2004). Gradual climate change and extreme events have already caused range shifts for some plant species (Chen et al., 2011), including range contraction with long-term population declines and extinctions (Lennartsson and Oostermeijer, 2001; Doak and Morris, 2010; Selwood et al., 2015, Wiens, 2016), or range expansion (Meer et al., 2016; Williams et al., 2015). This change is expected to become an even more important driver of global biodiversity loss over the next century (Heller and Zavaleta, 2009). Thus, population dynamics of many plant species are expected to be significantly affected by such changes (Breda et al., 2006; Meer et al., 2016; Nicolè et al., 2011; Ulrey et al. 2016). For conservation purposes, identifying climatic factors that impact population dynamics and predicting the consequences of climate change on species persistence have therefore become an important prerequisite to develop effective conservation strategies aimed at limiting population decline and extinction risk (Cotto et al., 2017; Malcolm et al., 2006; Thomas et al., 2004).

Climate change can either positively or negatively affect population dynamics (Lawson et al., 2015; Marrero-Gómez et al., 2007). For instance, climate change proved beneficial to populations of the widespread orchid species (*Orchis purpurea*) and is predicted to induce range expansion in the near future (Meer et al., 2016; Williams et al., 2015). In contrast, several studies have documented negative effects of summer temperature on growth rates for other plant species (Aragón-Gastélum et al., 2017; Riba et al., 2002; Shryock et al., 2014). In some cases, a given climatic variable has been shown to have diverging effects on separate vital rates within a species life-history (Csergő et al., 2017; Jolls et al., 2015; Nicolè et al., 2011; Peñuelas et al., 2004; Treurnicht et al., 2016). For example, a warm summer increased the flowering probability of *Dracocephalum austriacum*, whereas it decreased plant survival, leading to reduced effects of climate on population growth rates (Nicolè et al., 2011). Such opposite effects on population dynamics and demographic processes make it difficult to predict the net consequences of climate change on population viability (Meer et al., 2016; Nicolè et al., 2011).

2

55   The Mediterranean region has been identified as one of the most sensitive regions to
56   climate change (Ducrocq, 2016). Climate model projections indicate that warming and drying will
57   likely continue (AllEnvi, 2016). At the end of the century (2080-2099 period), annual mean
58   temperature is predicted to increase (+3.5°C) with more extreme dry event frequency (+46%) in this
59   region (Christensen et al., 2007). Moreover, in most areas of the Mediterranean region, precipitation
60   is predicted to decrease (-12%), particularly in summer (-24%, Christensen et al., 2007). The
61   Mediterranean region harbors an exceptional biodiversity, including a large number of rare and
62   endemic plant species. Among them, 36% are narrow endemics, i.e., they grow only in a single area
63   or have a narrow geographic range (Thompson et al., 2005). Most of these species occur in rocky
64   habitats, on steep slopes and in open vegetation with low species richness (Lavergne et al., 2004;
65   Thompson et al., 2005). Such habitats are characterized by their stability both in relation to
66   vegetation succession and human disturbance (Lavergne et al., 2005). Narrow endemic species are
67   expected to be particularly sensitive to environmental shifts, as several of these species are
68   extremely specialized and have evolved low dispersal ability (Isik, 2011; Lavergne et al., 2004,
69   2005; Thuiller et al., 2005).

70   Projection models that incorporate temporal environmental stochasticity are a powerful tool
71   for predicting long-term population dynamics under climate change (Andrello et al., 2012; Crone et
72   al., 2011, 2013; García et al., 2002). An increase in variability in vital rates due to climatic
73   variations will usually decrease the long-term population growth (Morris et al., 2008). Thus,
74   temporal variations may amplify population fluctuations and thus increase extinction risk, an effect
75   being more pronounced for small populations (Isik et al., 2011; Lande et al., 2003; Morris and Doak,
76   2002). Species life-histories can however buffer the effects of climate variation. For instance, long
77   duration of the life-cycle has been shown to decrease the impact of environmental stochasticity,
78   making long-lived species facing climate change less prone to extinction (Morris et al., 2008).
79   Demographic stochasticity can also be an important driver of population dynamics, whenever
80   populations are of a small size (Lande et al., 2003). Such processes refer to chance events of
81   individual survival and reproduction causing random variations in population growth rates (Caswell,
82   2001; Lande et al., 2003). These variations are expected to be more pronounced in small
83   populations and thus lead to random fluctuations in population size that increase extinction risks
84   (Lande et al., 2003; Zeigler, 2013). Including both environmental and demographic stochasticity in
85   population viability analyses is thus crucial to forecast the fate of populations under climate change
86   (Crone et al., 2011, 2013; Kaye and Pyke, 2003; Lande et al., 2003).

87   Demographic studies investigating the long-term effect of climate change on narrow
88 endemic Mediterranean plants remain rare. Such studies have mostly relied on short-term surveys,
89 thus exploring limited year-to-year climatic variations (Crone et al., 2011) and consider only a
90 subset of extant populations (e.g. *Centaurea hyssopifolia*; Matesanz et al., 2009, *Brassica insularis*;
91 Noel et al., 2010, *Ramonda myconi*; Riba et al., 2002), making it difficult to predict species
92 responses to climate change (Crone et al., 2011; Ehrlén et al., 2016). Long-term demographic
93 surveys are needed to understand how past climatic variations have affected population dynamics,
94 and to predict population viability under climate change (Andrello et al., 2012; Franklin et al., 2017;
95 Hunter et al., 2010; Menges, 2000). Typically, at least 15–20 years of observations are necessary to
96 predict population growth rate or extinction risk adequately (Zeigler, 2013). This is particularly true
97 for perennial species, which may have a stage in their life-cycle that allows for species persistence
98 under unfavorable conditions (Blume-Werry et al., 2016; Huelber et al., 2016; Morris et al., 2008).

99   *Centaurea corymbosa* is a narrow monocarpic short-lived species endemic to the
100 Mediterranean region. The species grows in the Massif de la Clape in Southern France, on the top
101 of cliffs and in nearby rocky areas of open vegetation (Colas et al., 1997). Only six populations are
102 known, which have been surveyed since June 1994 using permanent plots. In this paper, we used
103 this unique demographic dataset collected during a 22-year period (totaling 6112 individual life-
104 histories) to predict species dynamics under different climate scenarios. To do so, using matrix
105 population models, we estimated asymptotic growth rates and vital rates for each population and
106 each pair-of-years over the 22-year period. First, we tested for spatial and temporal variations in
107 population dynamics and also tested whether small populations had lower asymptotic growth rate
108 and showed higher variance in asymptotic growth rate than large populations. In addition, we tested
109 whether age at flowering could buffer the effects of environmental stochasticity. Next, we assessed
110 the relationship of climatic variables with demographic parameters over the 22-year period. More
111 specifically, we tested whether any climatic situation contributing to drought negatively affected
112 asymptotic growth rates and vital rates, since water availability is essential for the establishment of
113 newly recruited plants and the survival of vegetative plants. Moreover, because flowering is closely
114 linked with size and thus with plant growth in monocarpic plants (Meer et al., 2016; Metcalf et al.,
115 2003; Williams et al., 2015), we tested whether probability of flowering depended on climatic
116 conditions prevailing only the months before flowering or varied according to a cumulative multi-
117 year climate effect. Finally, by incorporating both environmental and demographic stochasticity, we
118 simulated the fate of populations under two climatic scenarios, a warm scenario reflecting an
119 increase in the frequency of hot years, and a dry scenario corresponding to an increase in the

4

120 frequency of drought events, and thus tested which of the two scenarios would have the largest
121 impact on population persistence.

2. Materials & Methods

2.1. Biological model, demographic and climatic datasets

2.1.1. Study species

125   *Centaurea corymbosa* Pourret (Asteraceae) is a narrow Mediterranean species endemic to
126 the Massif de la Clape near Narbonne (southern France, 43°13 N, 3°08 E). It is listed in the French
127 Red Book of endangered species and in the European Habitat Directive list of priority species, thus
128 precise coordinates of the populations are not given. *C. corymbosa* has been extensively studied
129 since 1994 and several papers have already reported on its ecological characteristics (Colas et al.,
130 1996; Imbert, 2006; Imbert et al., 2012; Kirchner et al., 2005), population dynamics (Fréville et al.,
131 2004; Kirchner et al., 2006) and population genetics (Colas et al., 1997, 2001; Fréville et al., 2001;
132 Fréville et al., 1998; Hardy et al., 2004; Riba et al., 2005). Here, we only summarize the most
133 important features and results related to the current study. *C. corymbosa* is restricted to a 3-km² area
134 and is known from only six populations found on different cliffs 0.3-2.3 km apart (mean elevation
135 132 m, SD = 37.4, n=41 permanent plots, see below). Individuals grow on the top of cliffs and in
136 rocky areas. These populations are currently not directly threatened by human activities. However,
137 habitat closure due to the abandonment of grazing contributes to the isolation of open and suitable
138 habitats, and thus increased fragmentation among patches. The species has a monocarpic perennial
139 life-cycle. Individuals stay as a rosette for 2 to 13 years before flowering. The flowering period
140 extends from May to mid-August, and most of the seeds germinate between September and
141 December. Seeds are dispersed over short distances by wind and ants. Despite suitable habitats in
142 the vicinity of the six populations, it has been shown that *C. corymbosa* is very unlikely to colonize
143 new sites (Colas et al., 1997; Olivieri et al., 2016; Riba et al., 2005).

2.1.2. Demographic dataset

145   Data have been collected since June 1994 in the six populations. However, in the first
146 census, the status of non-flowering plants (seedling or rosette) could not be assessed. Thus, matrix
147 population models were based on 22 years of demographic survey (1995-2016), except for one
148 population (Portes, 1996-2016). Data collection is described in details in Fréville et al. (2004).
149 Every 3 months (June, September, December and March), we recorded the presence and the status

150   of each individual within 41 permanent plots and new seedlings were added to the datasets (see

151   Appendix A1). During the flowering period (mid-June), we also surveyed the whole distribution

152   area of the species to count the total number of flowering plants per population (exhaustive count,

153   Table 1 and Appendix A2). A total of 6112 individual life-histories were used to construct

154   population projection models (Table 1 and Appendix A1).

155   *2.1.3. Climatic dataset*

156   Climatic data were obtained from the closest meteorological station located at INRA Pech

157   Rouge (43°1444 N, 3°1338 E, elevation = 40 m) less than 5 km from the populations of *C.*

158   *corymbosa*. We used daily mean temperature, daily minimum and maximum temperatures and daily

159   precipitation. Over the 22 years of this study, the Massif de la Clape experienced a classical warm

160   Mediterranean climate (average mean temperature 15.1 ± 0.6 °C from June *t* to May *t+1*, Fig. 1)

161   with a warm summer period. Precipitation regime was also characteristic of the Mediterranean

162   climate with an average of 540.8 mm per year from June *t* to May *t+1* with large inter-annual

163   variation (SD = 175.46, Fig. 1). The number of days with precipitation > 1 mm ranged from 35 days

164   to 68 days with an average of 48.5 days per pair-of-years (SD = 8.9, Fig. 1).

165   *2.2. Deterministic analyses*

166   *2.2.1. Matrix projection models*

167   As described in Fréville et al. (2004), the life-cycle is based on a prebreeding census

168   performed before the germination pulse, with a one-year interval from June *t* to May *t+1*. Three

169   stages were defined: seedlings (individuals less than 1 year old), rosettes (vegetative plants older

170   than 1 year), and flowering plants. We estimated lower-level vital rates (survival s_i, flowering

171   probability α_i conditional to survival and fecundity f) to construct a stage structured Matrix

172   Projection Model (MPM). For each population and each pair-of-years, the projection matrix

173   representing the life-cycle is given by:

$$A = \begin{pmatrix} 0 & 0 & fs_0 \\ s_1(1-\alpha_1) & s_2(1-\alpha_2) & s_3(1-\alpha_3) \\ s_1\alpha_1 & s_2\alpha_2 & s_3\alpha_3 \end{pmatrix}$$

174   From the 22 years of demographic survey, we constructed 21 matrices per population (see

175   appendix B for projection matrices per population). The probabilities of a flowering plant to survive

176   (s_3) and to reproduce the year after (α_3) were very low, in agreement with the monocarpy of the

6

species, and had negligible effects on population dynamics (see appendix B). Using a deterministic MPM (linear, time-invariant), we calculated the asymptotic growth rate λ_a as the dominant eigenvalue of the matrix **A** of the corresponding pair-of-years. The model did not include seed bank and migration. Indeed, less than 5% of seeds may remain dormant for one year and seed dispersal among populations is highly limited (Colas et al., 1997; Fréville et al., 2004; Imbert, 2006). The net fecundity fs_0 was estimated as the ratio of the number of seedlings observed in June of a given year over the number of flowering plants observed within permanent plots in June of the previous year. Our three-month survey made it possible to decompose the net fecundity fs_0 into a fecundity term f (number of just-emerged seedlings assessed every three months over number of flowering plants in June t-1) and survival of just-emerged seedlings s_0 (number of seedlings observed in June t over total number of just-emerged seedlings observed from June t-1 to May t, Colas et al., 2008; Fréville et al., 2004). We obtained four null values in asymptotic growth rates (three for Cruzade and one for Peyral), which corresponded to years with no flowering plant within plots and null values in rosette survival s_2. In such case, the persistence of the plot depended on new rosettes coming from the seedling stage (s_1 never equaled zero), and seed dispersal from the closest flowering plants outside plots. When calculating the geometric mean of asymptotic growth rates over years for each population, we excluded these null values.

2.2.2. Patterns of spatio-temporal variations in asymptotic growth rates

To test for temporal and spatial variation in asymptotic growth rates, we used non-parametric randomisation tests (Caswell, 2001). Temporal variation was tested by randomly permuting individual life-histories (status at t and fate at t+1) among pair-of-years when considering all data as a single population. For spatial variation, we permuted the whole individual life-history (from germination to death) between populations (see Fréville et al., 2004). Each life-history appeared exactly once in each randomized dataset, maintaining the original sample sizes. For each set of permuted data, we calculated asymptotic growth rate for each group (year or population) and then computed the standard deviation of λ_a between groups. The probability that $\sigma(\lambda_a) \geq \sigma_{obs}$ under the null hypothesis H_0 (no group effect) was computed based on 2000 random permutations. We rejected H_0 when this probability was smaller than 0.05 (Caswell, 2001). We used linear models to test for the effect of population size on asymptotic growth rates and their temporal variance, using the total number of flowering plants obtained by the exhaustive survey as a proxy of population size (Table 1). We used also a linear model to test for the effect of mean age at flowering (Table 1) on the variance in population growth rate.

7

209 *2.2.3. Retrospective and prospective analyses*

210   We performed a life-table response analysis (LTRE) with a random design to assess how
211 lower-level vital rates contributed to the variance in asymptotic growth rates var(λ_a) observed
212 among years. This analysis was performed on the pooled data over populations, provided that we
213 did not detect significant spatial variation in population growth rates. The decomposition of var(λ_a)
214 in term of lower-level vital rates *p* is expressed as:

$$var(\lambda_a) \approx \sum_{i,j} cov(p_i,p_j) \frac{\partial \lambda_a \partial \lambda_a}{\partial p_i \partial p_j}$$

215 where $cov(p_i,p_j)$ is the covariance of p_i and p_j (Caswell, 2001). A prospective analysis was also
216 conducted to assess the population dynamic response to changes in lower-level vital rates. We
217 calculated the elasticity of λ_a to lower-level vital rates *p* as:

218
$$e = \frac{p}{\lambda_a} \frac{\partial \lambda_a}{\partial p}$$

219 *2.3. Relationships between demographic parameters and climate*

220   From the raw climatic dataset, we extracted seven relevant variables assumed to have an
221 influence on demographic parameters, given the existing literature (Fréville et al., 2004; Riba et al.,
222 2002) and our knowledge of Mediterranean plant species. We thus calculated the average of daily
223 mean temperature and daily maximum temperature, the number of days with mean T° > 25°C
224 (corresponding to mean + SD) and the number of freezing days (minimum T° < 0°C). In addition,
225 we calculated both the average cumulative precipitation and the number of days with precipitation >
226 1 mm that hereafter will be referred as the number of wet days. We also calculated the number of
227 days with precipitation > 20 mm. This threshold value was equal to mean + SD. We thus considered
228 this variable as reflecting the number of heavy precipitation events in the Massif de la Clape.

229   We tested for the effect of climate on demographic parameters using generalized linear
230 models with identity link for asymptotic growth rates and fecundity *f* (both log-transformed), and
231 logit link for survival and flowering probabilities with the binomial distribution. First, we tested for
232 relationships between annual averages of each climatic variable calculated from June *t* to May *t+1*
233 and asymptotic growth rates λ_a, and also tested for quadratic effects and multiyear cumulative effect
234 with a time lag of one year of each climatic variable (Appendix E.1). We then tested for the effect
235 of the variables that we found significant in the single-variable GLMs, using a forward stepwise

8

236   selection approach. Starting from the null model, we added at each step the variable having the

237   highest R^2 value in the single-variable models (Appendix E.1). For logistic models, we used R^2_{LR},

238   the pseudo-coefficient of determination based on the likelihood-ratio test and given by $R^2_{LR} = 1-$

239   $(L_{null} /L_{full})^{2/n}$ where L_{null} and L_{full} are the likelihoods of the null and the fitted models, respectively

240   (Shinichi Nakagawa et al., 2013). The significance of each added variable in the model was tested

241   using an analysis of deviance (Appendix E.2). From the best model, we reported the estimated

242   coefficient (β) and its significance for each variable in the model after scaling climatic variables.

243   Second, to understand biological processes at a finer scale, we tested for the impact of the seasonal

244   climate on lower-level vital rates by considering only climatic variables that significantly impacted

245   asymptotic growth rates, using the same approach as described above. We included the seasonality

246   effect in GLMs by averaging variables over three-month periods separating two successive censuses

247   (Appendix E.3). GLMs were fitted using R Stats-package (version 3.3.1). The R^2_{LR} was calculated

248   using the R-command 'r.squaredLR' from the MuMIn-package (version 1.15.6).

249   *2.4. Stochastic projections under climate change*

250   Based on the IPCC Fourth Assessment Report, the frequency of extreme warm and dry

251   events is expected to increase (Christensen et al., 2007). We thus built stochastic matrix models to

252   simulate the fate of *C. corymbosa* populations under two scenarios of climatic variations,

253   representing an increased frequency of extreme events either for temperature or precipitation

254   (Bucharovà et al., 2012; Shryock et al., 2014). To simulate the fate of populations, we incorporated

255   environmental stochasticity by drawing an entire matrix at each time step (sampling with

256   replacement) among the 21 available matrices (Crone et al., 2011, 2013; Kaye and Pyke, 2003).

257   Because *C. corymbosa* has small population sizes, we also incorporated demographic stochasticity

258   in the models. Such stochasticity is due to the independent chance of transition and reproduction

259   among individuals (Engen et al., 1998; Lande, 1993; Melbourne and Hasting, 2008). From the

260   existing individuals at year *t,* we drew the number of individuals making each transition from stage

261   *j* to stage *i* including death at each time step in a multinomial distribution characterized by the a_{ij}

262   transition probabilities of the matrix that we randomly drew (Andrieu et al., 2017; Caswell, 2001;

263   Melbourne and Hasting, 2008; Morris and Doak, 2002). The number of recruited seedlings was

264   drawn in a Poisson distribution with mean equal to the fs_0 value of the drawn matrix. In the case of

265   *C. corymbosa*, demographic stochasticity indeed increased fluctuations in population size over time

266   and thus increased extinction risk (see Appendix F), in agreement with both theoretical studies (e.g.

267   Engen et al., 2005; Lande, 1993; Lande, 2003) and empirical ones (e.g. Fujiwara and Caswell, 2001;

9

268 Melbourne and Hasting, 2008; Jepsonn and Forslund, 2012). Therefore, we combined both
269 demographic and environmental stochasticity to simulate the fate of populations under climate
270 scenarios.

271   The initial population size N_0 used to start our simulations was calculated from the stable
272 stage distribution obtained from the arithmetic mean of the total number of flowering plants
273 recorded in the population (exhaustive survey) from 2010 to 2016, and the scaled eigenvector W
274 from the arithmetic mean matrix over years (2010-2016) when pooling data over populations. N_0 is
275 given by $N_0 = W \frac{Nfr}{w_3}$ where w_3, the third element of the scaled eigenvector, represents the
276 proportion of the number of flowering plants. We simulated population dynamics using 1000
277 stochastic iterations, each iteration representing a trajectory of population size over 100 years. For a
278 given trajectory we calculated the growth rate λ_j as:

$$\lambda_j = exp\left[\frac{ln(n_j(T)) - ln(n_j(0))}{T}\right]$$

279 where $n_j(T)$ and $n_j(0)$ were the population size of the jth trajectory at $t = T$ and $t = 0$, respectively,
280 and T being the last year at which population size was non-null. The stochastic growth rate λ_s was
281 obtained as the median of λ_j over 1000 trajectories. Extinction probability at a given time t
282 corresponds to the number of trajectories for which $N(t) = 0$ over the total number of trajectories;
283 we calculated extinction probability at $t = 50$ years (P_{50}), $t = 100$ years (P_{100}) and the mean time to
284 extinction (T_{ext}) based on 100 trajectories over 100 years. We carried out 1000 such simulations,
285 each of 100 trajectories, to obtain a sampling distribution of P_{50}, P_{100} and T_{ext}. We calculated mean
286 value of those parameters over the 1000 simulations and 95% confidence intervals by taking the
287 2.5[th] and the 97.5[th] percentile of the simulated distribution (Shryock et al., 2014). All stochastic
288 analyses were implemented using the R popbio-package, version 2.4.3 (Stubben and Milligan,
289 2007).

290   Climatic scenarios were first simulated by increasing the frequency of drawing matrices
291 corresponding to extreme warm and extreme dry years (Andrello et al. 2012; Hunter et al., 2010;
292 Shryock et al., 2014) from the observed frequency over the 22-year period q* to q = 0.8, that
293 represent, respectively, the warm and the dry scenario. Based on the results of the GLM analyses
294 testing for the effects of climatic variables on asymptotic growth rates, we used the daily mean
295 temperature and the number of wet days to characterize warm and dry scenarios, respectively.

296 Following Williams et al. (2015), extreme years corresponded to years with climate values larger
297 than one standard deviation above the daily mean for temperature and lower than one standard
298 deviation below the mean for precipitation. In the warm scenario, warm years were represented by
299 pair-of-years with high daily mean temperature (2006-2007, 2013-2014, 2014-2015 and 2015-2016,
300 Fig. 1, $q^*=4/21=0.19$). In the dry scenario, dry years were represented by pair-of-years with low
301 numbers of wet days (2001-2002, 2006-2007 and 2010-2011, Fig. 1, $q^*=3/21=0.14$).

302 Second, following the approach described in Salguero-Gomez et al. (2012), we focused on
303 a particular climate scenario resulting from the Regional Climate Model (RCM) proposed by the
304 Euro-Cordex 2014 project (Jacob et al., 2014). We used the RCP4.5 scenario representing an
305 intermediate scenario of increasing CO_2 concentration until 2060. The regional climate model
306 simulations provided predicted values of daily precipitation and mean temperature. We then
307 extracted these data for the closest geographic location, which is less than 1 km apart from the
308 centroid of the species distribution (43.13710 N, 3.07327 E) and less than 6 km apart from the
309 meteorological station we used to get observed climatic data. Overestimation of precipitation in
310 RCMs is a well-known problem, in particular in areas close to the Mediterranean Sea (Gao et al.,
311 2008; Ruffault et al., 2014). Therefore, to estimate the frequency of extreme years in the future
312 (2020-2099), we used threshold values from the back-projected model values (Salguero-Gomez et
313 al., 2012). Using the back-projected data from the reference period (1971-2005), we defined warm
314 years as those with mean temperature from May t to June $t+1$ greater than 14.5 + 1.23 (mean + SD)
315 and dry years as those with number of wet days lower than 68.6 - 14.8 (mean - SD). Comparing the
316 observed data and the back-projected data for the overlapping period 1995-2005, we indeed
317 document an overestimation of the number of wet days predicted by the regional model compared
318 to the observed one (paired t-test = 4.57, df = 8, $p < 0.002$). In contrast, predicted and observed
319 daily mean temperatures and total precipitation were not significantly different ($p > 0.10$).
320 Simulated data are available on the Drias platform (www.drias-climat.fr).

321 **3. Results**

322 *3.1. Patterns of spatio-temporal variations in asymptotic growth rates*

323 Asymptotic growth rates λ_a calculated per population and per pair-of-years showed a
324 decreasing trend over time (β = - 0.01, p = 0.02, Fig. 2A). The slope of the trend for each population
325 separately was significant only for the smallest population (Cruzade: β = -0.04; p = 0.01, Fig. 2D).
326 When pooling populations within each pair-of-years, the geometric mean of asymptotic growth

11

rates over years was 0.880 (Table 1), with λ_a ranging from 0.432 (2006-2007) to 1.815 (2012-2013). Geometric means of λ_a over years per population were all lower than 1 and varied between 0.710 (Peyral) and 0.836 (Enferret1, Table 1). No significant relationship was detected between asymptotic growth rate and population size ($\beta = 0.0003$; $p = 0.46$). Randomization tests showed that the difference in λ_a among years was highly significant ($p < 0.001$, see appendix C). In contrast, asymptotic growth rates λ_a were not significantly different among populations ($p = 0.16$, see appendix C). The variance in λ_a per population was not significantly correlated with mean age at flowering ($\beta = -0.02$; $p = 0.68$) nor with population size ($\beta = 0.0003$; $p = 0.55$).

3.2. Retrospective and prospective analyses

As λ_a did not differ significantly among populations, retrospective and prospective analyses were performed after pooling individuals across populations. The observed variance in asymptotic growth rates among years was equal to 0.083, and was mainly explained by the variation in both the fecundity term (f), the survival of seedlings (s_1) and the survival of rosettes (s_2) having the highest contributions (0.025, 0.023 and 0.021, respectively, Fig. 3), followed by the survival of just-emerged seedling (s_0) and the flowering probability of rosettes (α_2) having a similar contribution (0.008, Fig. 3). Rare events in the life-cycle (flowering probabilities α_1 and α_3, and survival of flowering plants s_3) had negligible contributions (sum to 0.0009, Fig. 3 and appendix D). The largest elasticity of asymptotic growth rate was associated with rosette survival (s_2) followed by the fecundity term f (mean number of just-emerged seedlings per flowering plant), the survival of just-emerged seedling (s_0), seedling survival (s_1) and the flowering probability of rosettes (α_2, Fig. 3). Elasticity of λ_a to the remaining lower-level vital rates representing rare events (s_3, α_1 and α_3) summed only to 1% (Fig. 3). These latter rates were thus not considered for the GLMs investigating the relationship between lower-level vital rates and climatic variables.

3.3. Relationship between asymptotic growth rates and climate

Asymptotic growth rate, when pooling populations, was best explained by a model including only two climatic variables ($R^2 = 0.58$, Appendix E.2), with a high positive effect of the annual number of wet days ($\beta = 0.15$, $p = 0.004$) and a negative effect of the annual average daily mean temperature ($\beta = -0.11$, $p = 0.03$). The number of freezing days, the cumulative precipitation and the number of days with precipitation > 20 mm proved non-significant ($p > 0.05$, Appendix E.1). No multiyear cumulative effect and no quadratic effect of climatic variables were significant ($p > 0.05$, Appendices E.1).

12

3.4. Relationships between lower-level vital rates and climate

Overall, warming and drought negatively affected vital rates. The mean number of just-emerged seedlings per flowering plants f was negatively impacted by the daily mean temperature during both summer and fall periods (Table 2). The survival of just-emerged seedlings s_0 was positively impacted by the number of wet days during the germination period (both fall and the winter periods), and negatively impacted by the daily mean temperature during both summer and fall periods (Table 2). Seedling survival s_1 was negatively affected by an increase in the daily mean temperature during the summer and fall periods, and positively affected by an increase in the number of wet days during the same periods (Table 2). Rosette survival s_2 decreased with increasing summer daily mean temperature (Table 2). Finally, the flowering probability of rosettes α_2 was negatively impacted by the summer daily mean temperature and positively impacted by the number of wet days during the fall period (Table 2).

3.5. Stochastic projections under climate change

In absence of climate change, when randomly drawing each matrix with equal probability (1/21), stochastic growth rates λ_s were significantly lower than 1 when pooling populations (λ_s = 0.881, *CI* = [0.877, 0.889], Table 1). Stochastic growth rates were also lower than 1 in each population, ranging from 0.742 for the smallest population Cruzade (*CI* = [0.732, 0.770]) to 0.836 for the largest one Enferret2 (*CI* = [0.829, 0.851], Table 1).

To assess the combined effect of environmental and demographic stochasticity on population viability, we compared the fate of the smallest population Cruzade and the largest one Enferret2, using their respective population size at $t = 0$ (see details above and Fig. 4). As we did not detect any significant variation in asymptotic growth rates among populations, we pooled data across population for each pair-of-years to obtain the 21 matrices used to simulate climate change. In the warm scenario, when increasing the frequency of extreme years from q* (4/21 = 0.19) to 0.8, stochastic growth rates decreased from 0.882 to 0.761 for the largest population (Enferret2, Fig. 4A) and from 0.879 to 0.765 for the smallest one (Cruzade, Fig. 4C). Under the RCP4.5 scenario, the predicted frequency of warm year q_{pred} characterized by a daily mean temperature > 15.63 °C for the period 2020-2099 equaled 0.78 and led to the extinction of both populations at 100 years in most simulations (Figs. 4A and 4C, solid black lines). Comparing this scenario with those of no climate change (Figs. 4A and 4C, dashed green lines), extinction probability at 50 years (P_{50}) increased from 0.37 to 0.99 for Enferret2 and from 0.82 to 0.99 for Cruzade, while extinction

13

389 probabilities at 100 years (P_{100}) were close or equal to 1 for both populations. The mean time to
390 extinction decreased from 57 to 26.4 years for Enferret2, and from 32 to 16 for Cruzade.

391 The dry scenario had less dramatic consequences on the viability of populations than the
392 warm scenario (Fig. 4B and 4D). The increase in dry year frequency from q* (3/21=0.14) to 0.8 led
393 to a small reduction in λ_s from 0.882 to 0.855 for Enferret2 and from 0.879 to 0.851 for Cruzade
394 (Figs. 4B and 4D, respectively). The RCP4.5 scenario predicted a frequency of dry years q_{pred},
395 corresponding to a number of wet days lower than 53.8 days, equaled to 0.15, a value very close to
396 the one observed during the 22-year period of our demographic survey. The RCP4.5 scenario did
397 not result in any significant change in extinction probabilities and mean time to extinction compared
398 to the scenario of no climate change, whatever the size of populations (Figs. 4B and 4D, solid black
399 lines).

400 **4. Discussion**

401 *4.1 Long term population dynamics of Centaurea corymbosa*

402 Our results demonstrate the need for long-term demographic surveys to better understand
403 the spatio-temporal demographic variability on plants (Blume-Werry et al., 2016; Compagnoni et
404 al., 2016; Crone et al., 2011; Huelber et al., 2016). Indeed, our study based on 22 years of data
405 provided a more accurate picture of the determinants of population dynamics in *C. corymbosa* than
406 the study of Fréville et al. (2004) based on 8 years of data. In Fréville et al. (2004), the standard
407 deviation in asymptotic growth rates $\sigma(\lambda)$ was 0.116 among years and 0.099 among populations,
408 with significant differences among years and populations. In the current study, variation among
409 populations became non-significant and temporal variation in asymptotic growth rates was rather
410 synchronized among populations (Fig. 2). This pattern is not surprising given the narrow
411 distribution of *C. corymbosa* and is largely consistent with studies of other narrowly distributed
412 species (Buckley et al., 2010; Kiviniemi and Löfgren, 2009; Ramula et al., 2008). More importantly,
413 the standard deviation $\sigma(\lambda)$ observed over the 22-year period was much larger (0.230) than the one
414 (0.116) reported in Fréville et al. (2004). In agreement with the results of the permutation tests, we
415 did not find any significant correlation between population dynamics and population size. Indeed,
416 we did not find any evidence that small populations had lower population growth rates. Moreover,
417 the variance in asymptotic growth rates among years did not increase with decreasing population
418 size. In contrast to other demographic studies (Lande et al., 2003; Zeigler, 2013), we thus did not
419 find any evidence of a greater sensitivity of the smallest populations to both environmental and

14

420 demographic stochasticity in our species. In addition, the variance in asymptotic growth rate was
421 not correlated with mean age at flowering per population. We thus did not find evidence for
422 demographic buffering in populations with greater longevity, in contrast to what has been found at
423 an inter-specific scale in Morris et al. (2008). Population dynamics of *C. corymbosa* is thus mainly
424 affected by environmental factors that vary over time rather than by spatial factors.

425   Average and most of the yearly asymptotic growth rates were lower than 1 for each
426 population and when pooling individuals across populations. Overall, we observed a declining trend
427 in yearly asymptotic growth rates over the 22-year period (Fig. 2), this trend being significant for
428 the smallest population and when considering all populations (Figs. 2A and 2D, respectively).
429 Asymptotic growth rates were negatively impacted by an increase in temperature and positively
430 impacted by the number of wet days. Consistent with these results, asymptotic growth rates attained
431 extreme values in years corresponding to extreme climatic events. Indeed, when pooling all
432 individuals in a single population, the lowest value (0.432, Fig. 2A) was observed in 2006-2007
433 when the mean temperature was the highest (16.3° C, Fig. 1) and the number of wet days was the
434 lowest (34 days, Fig. 1). The highest growth rate (1.815, Fig. 2A) corresponded to 2012-2013, when
435 we observed the second lowest mean temperature (14.2° C, Fig. 1) and the highest number of wet
436 days (66 days, Fig. 1). Thus, population dynamics of *C. corymbosa* was mainly affected by extreme
437 climatic events, which are predicted to increase in the future. Climatic variables investigated here
438 did not show any marked temporal trend over the 22-year period of our demographic survey (Fig.1),
439 which could explain the weak temporal trend observed in asymptotic growth rates. Overall, our
440 study confirms that extreme climatic events are an important driver of plant population dynamics as
441 reported in other studies (Andrello et al., 2012; Davison et al., 2010; McDowell et al., 2008;
442 Shryock et al., 2014; Ulrey et al., 2016).

443   In contrast to some studies reporting both negative and positive effects of climate change
444 on vital rates (Meer et al., 2016; Meisner et al., 2014; Nicolè et al., 2011), our study documents a
445 consistent negative effect of increased temperature and drought on lower-level vital rates in *C.*
446 *corymbosa*. Regarding temperature, the most critical season that impacted lower-level vital rates
447 was the summer period, since increasing summer daily mean temperature negatively affected both
448 fecundity, survival probability and flowering probability. In contrast to our study, flowering
449 probability was found to be positively impacted by high temperature in some temperate plant
450 species (e.g. *Himantoglossum hircinum*, Meer et al., 2016; *Dracocephalum austriacum*, Nicolè et
451 al., 2011). While a negative effect of increasing temperature on flowering probability was also

15

452   reported in Peñuelas et al. (2004), this pattern was only observed in the southern Mediterranean
453   sites but not in the northern ones. A likely explanation of this negative effect is that warm summers
454   increase evapo-transpiration and decrease soil moisture (Christensen et al., 2004; Peñuelas et al.,
455   2004). This could lead to a decrease in plant biomass as a consequence of rosette shrinking that in
456   turn reduces the amount of resources that a plant can allocate to reproduction (Manders and Smith,
457   1992). This is particularly true for monocarpic perennial species, where flowering probability has
458   been shown to increase with plant size (Metcalf et al., 2003). Regarding precipitation, the youngest
459   plants were the most impacted by the number of wet days. This factor had a positive effect on both
460   survival of just-emerged seedlings (s_0) during the germination period (fall and winter) and seedling
461   survival (s_1) during the summer and fall periods, which is consistent with several studies showing a
462   positive impact of the frequency of wet days (Riba et al., 2002; Shriver, 2016). Both temperature
463   and precipitation effects may be explained by the fact that recurrent warm and dry days can induce
464   a seasonal water deficit, which may negatively impact the whole life-cycle (Manders and Smith,
465   1992; Peñuelas et al., 2004; Ruffault et al., 2014). Species growing in rocky habitats, such as *C.*
466   *corymbosa*, are likely to be the most affected, since these soils have a very low water capacity
467   (Ruiz-Sinoga et al., 2012; Silva et al., 2015). Moreover, herbaceous species such as *C. corymbosa*
468   do not have a deep root system ensuring access to water over dry periods in such rocky habitats.

469   *4.2 Predictions from climate scenarios*

470   Both demographic and environmental stochasticity are important factors in determining the
471   viability of species with small population sizes (Caswell, 2001; Crone et al., 2013; Garcia et al.,
472   2002). We here showed that climate variation explained a large amount of variation in vital rates
473   and growth rates in *C. corymbosa*. We thus used stochastic models to predict the fate of *C.*
474   *corymbosa* populations with both environmental stochasticity arising from climate change and
475   demographic stochasticity. We did not include density-dependence in our model, which could make
476   quantitative predictions overly pessimistic (Dahlgren et al., 2016). Population viability analyses are
477   acknowledged to be relevant tools to quantitatively compare the impact of different scenarios rather
478   than quantitatively predict the future status of populations (Coulson et al., 2001). We thus used
479   population viability analyses to compare how the warm and the dry scenarios impacted population
480   viability of *C. corymbosa* rather than attempting to explicitly predict future population size.

481   Stochastic projections predicted population declines ($\lambda_s < 1$) under no climate change.
482   Populations were predicted to decline even faster in the future in response to an increased frequency
483   of extreme years in both the warm and dry scenarios. Such results are consistent with the GLMs

16

484 showing negative impacts of warming and drought, and several studies investigating population
485 viability in response to climate change (Andrello et al., 2012; Lawson et al., 2015; Marrero-Gómez
486 et al., 2007; Shryock et al., 2014). More importantly, the warm scenario had more severe
487 consequences on population viability than the dry scenario whatever the initial population size.
488 However in our simulations, the initial population size impacted both extinction probability and the
489 mean time to extinction, a pattern consistent with theoretical studies since small populations are
490 more vulnerable to extinction than largest ones (Groom et al., 2005; Lande et al., 2003). Using the
491 RCP4.5 scenario, the change in temperature projected for the period 2071-2099 was of the same
492 order of magnitude than the one predicted by other regional climatic models (Christensen et al.,
493 2007; Ruffault et al., 2014). In contrast, our dry scenario predicted an annual mean number of wet
494 days equal to 66.41 (-3.2%), while other models predicted a much severe decrease (-19.6%,
495 Ruffault et al., 2014). This suggests that uncertainty in climate models should be carefully
496 considered in management plans and when evaluating extinction risk. Such uncertainty is
497 particularly pronounced for the Mediterranean region (Gao et al., 2008; Ruffault et al., 2014).

498 Faced with climate change, populations can either migrate or adapt by microevolution or
499 phenotypic plasticity to avoid extinction (Groom et al., 2005; Lande et al., 2003). In the
500 Mediterranean region, many narrow endemic species are characterized by a low ability to colonize
501 existing suitable habitats due to several biological traits such as low dispersal ability (Colas et al.
502 1997; Lavergne et al., 2004; Thompson et al. 2005). In *C. corymbosa*, self-incompatibility and
503 monocarpy make successful colonization even less likely (Colas et al., 1997). Thus, for such species,
504 persistence mainly depends upon their ability to respond plastically to climate change or to become
505 locally adapted to new environmental conditions (Cotto et al., 2017; Knight et al. 2008; Menges,
506 2000). Theoretical work suggests that perennial species should display slower evolutionary
507 responses than annual plants, since higher adult survival limits the adaptive capacity of local
508 populations (Cotto et al., 2017). Moreover, small populations have a lower evolutionary potential,
509 since they become genetically impoverished due to the impact of genetic drift. Using a shorter
510 survey (1995-2001), Fréville et al. (2001) showed that demographic rates were not correlated with
511 intra-population genetic diversity in *Centaurea corymbosa* (Fréville et al., 2001). Using the same
512 genetic data (Table 1 in Fréville et al., 2001), we likewise confirmed that genetic diversity was
513 correlated with neither λ_s (Spearman correlation *rho* = 0.26, p = 0.61) nor the slope of regression in
514 asymptotic growth rates over years (*rho* = 0.09, p = 0.89). Thus, our results do not support evidence
515 for accumulation of deleterious mutations (Lynch et al., 1995), nor a loss of standing variation due
516 to genetic drift in small populations of *C. corymbosa*.

17

4.3 Management recommendations

518   Persistence of narrow endemic species in the Mediterranean region may have been favored
519 by the capacity of those species to grow in rocky habitats (Thompson et al., 2005), since these
520 remote habitats do not face direct threats due to human activities. Demographic studies of cliff-
521 dwelling species have shown unusual demographic stability and resilience of these plants (García,
522 2003; Lavergne et al., 2005; Picó and Riba, 2002; Thompson et al., 2005), likely arising from much
523 higher importance of rosette survival than recruitment for the maintenance of populations (Cotto et
524 al., 2017; Larson et al., 2000; Silva et al., 2015). In a scenario of no climate change, rosette survival
525 (that had the highest elasticity on growth rates) should be increased from 0.71 to 0.92 to ensure the
526 persistence of *C. corymbosa* in a deterministic model (Appendix G). However, management actions
527 aimed at increasing specific vital rates, such as watering plants are not feasible in such rocky
528 habitats. Implementing management actions that reduce the negative effects of demographic,
529 genetic and environmental stochasticity by manipulating population size and population number
530 appear much more promising.

531   Previous studies have shown the importance of biological features such as self-
532 incompatibility and low dispersal ability on the population persistence of *C. corymbosa* (Colas et al.
533 1997). Two new populations were introduced in 1994 on the top of unoccupied cliffs thus
534 confirming the existence of suitable but empty habitats nearby existing natural populations (Colas et
535 al., 2008; Kirchner et al., 2006). Introduced populations exhibited on average higher plant survival
536 than natural populations, mainly because seeds had been introduced manually in a priori suitable
537 microsites (Colas et al. 2008). However, fecundity in introduced populations was lower than in
538 natural ones, likely as a consequence of low local density of flowering plants, leading to strong
539 pollen limitation (Colas et al. 2008). One introduced population has been extinct for 5 years, while
540 the other population only harbored 35 plants in the last census performed in December 2017. In the
541 future, protocols should be carefully designed to ensure successful introductions. For instance,
542 introducing a large number of seeds (>1000) distributed over a few sites and at yearly intervals
543 should allow population persistence on the short term (Colas et al., 2008; Kirchner et al., 2006).

544   Faced with accelerated climate change, conservation policies for endangered species, such
545 as *C. corymbosa*, should be reconsidered. As our study demonstrated the importance of climate on
546 the fate of populations, introductions in distant habitats should be considered, although such
547 assisted colonization event requires suitable and available habitats at a larger scale. At present,
548 prioritization actions of conservation rely on the climatic niche of the species (Jones et al., 2016;

18

549   Oliver et al., 2016), and depend on our ability to define new protected areas in Northern localities
550   (Araújo et al., 2011; Bellard et al., 2012) or microrefugia (i.e. location with a low impact of climate
551   change, Jones et al., 2016; Ulrey et al. 2016). Recently, an increasing amount of empirical evidence
552   has been gathered to document that organisms, including plants, can show microevolutionary
553   responses in natural populations (Franks et al., 2014; Thomann et al., 2013), suggesting plants can
554   adapt to new environmental conditions (Thompson et al., 2005). Therefore, reinforcement, which
555   allows increasing population size and thus reducing extinction risk arising mainly from
556   demographic and genetic stochasticity, is also potentially an efficient and reasonable management
557   strategy for species facing climate change.

Acknowledgments

567

568

Bibliography

AllEnvi (2016). The Mediterranean region under climate change (Paris: IRD Editions).

Andrello, M., Bizoux, J.-P., Barbet-Massin, M., Gaudeul, M., Nicole, F., and Till-Bottraud, I. (2012). Effects of management regimes and extreme climatic events on plant population viability in *Eryngium alpinum*. Biol. Cons. 147, 99–106.

Andrieu, E., Besnard, A., Fréville, H., Vaudey, V., Gauthier, P., Thompson, J.D., and Debussche, M. (2017). Population dynamics of *Paeonia officinalis* in relation to forest closure: From model predictions to practical conservation management. Biol. Cons 215, 51–60.

19

Aragón-Gastélum, J.L., Badano, E., Yáñez-Espinosa, L., Ramírez-Tobías, H.M., Rodas-Ortiz, J.P., González-Salvatierra, C., and Flores, J. (2017). Seedling survival of three endemic and threatened Mexican cacti under induced climate change. Plant Species Biol. *32*, 92–99.

Araújo, M.B., Alagador, D., Cabeza, M., Nogués-Bravo, D., and Thuiller, W. (2011). Climate change threatens European conservation areas. Ecol. Lett. *14*, 484–492.

Bellard, C., Bertelsmeier, C., Leadley, P., Thuiller, W., and Courchamp, F. (2012). Impacts of climate change on the future of biodiversity. Ecol. Lett. *15*, 365–377.

Blume-Werry, G., Kreyling, J., Laudon, H., and Milbau, A. (2016). Short-term climate change manipulation effects do not scale up to long-term legacies: effects of an absent snow cover on boreal forest plants. J. Ecol. *104*, 1638–1648.

Breda, N., Huc, R., Granier, A., and Dreyer, E. (2006). Temperate forest trees and stands under severe drought: a review of ecophysiological responses, adaptation processes and long-term consequences. Ann. For. Sci. *63*, 625–644.

Bucharová, A., Brabec, J., and Münzbergová, Z. (2012). Effect of land use and climate change on the future fate of populations of an endemic species in central Europe. Biol. Conserv. *145*, 39–47.

Caswell, H. (2000). Prospective and retrospective perturbation analyses: their roles in conservation biology. Ecology *81*, 619–627.

Caswell, H. (2001). Matrix population models: Construction, analysis, and interpretation (Sunderland, Mass: Sinauer Associates Inc.,U.S.).

Christensen, J.H., Hewitson, B., Busuioc, A., Chen, A., Gao, X., Held, R., Jones, R., Kolli, R.K., Kwon, W.K., Laprise, R., et al. (2007). Regional climate projections. In Climate Change, 2007: The Physical Science Basis. Contribution of Working Group I to the Fourth Assessment Report of the Intergovernmental Panel on Climate Change, University Press, Cambridge, (Cambridge University Press), pp. 848–940.

Christensen, L., Coughenour, M.B., Ellis, J.E., and Chen, Z.Z. (2004). Vulnerability of the Asian typical steppe to grazing and climate change. Clim. Change *63*, 351–368.

20

Colas, B., Riba, M., and Molina, J. (1996). Statut démographique de *Centaurea corymbosa* Pourret (Asteraceae), Hormatophylla pyrenaica (Lapeyr.) Cullen & Dudley (Brassicaceae) et Marsilea strigosa Willd. (Marsileaceae-Pteridophyta), trois plantes rares du sud de la France. Acta Bot. Gallica *143*, 191–198.

Colas, B., Olivieri, I., and Riba, M. (1997). *Centaurea corymbosa*, a cliff-dwelling species tottering on the brink of extinction: A demographic and genetic study. Proc. Natl. Acad. Sci. *94*, 3471–3476.

Colas, B., Olivieri, I., and Riba, M. (2001). Spatio-temporal variation of reproductive success and conservation of the narrow-endemic *Centaurea corymbosa* (Asteraceae). Biol. Cons. *99*, 375–386.

Colas, B., Kirchner, F., Riba, M., Olivieri, I., Mignot, A., Imbert, E., Beltrame, C., Carbonell, D., and Fréville, H. (2008). Restoration demography: a 10-year demographic comparison between introduced and natural populations of endemic *Centaurea corymbosa* (Asteraceae). J. Appl. Ecol. *45*, 1468–1476.

Compagnoni, A., Bibian, A.J., Ochocki, B.M., Rogers, H.S., Schultz, E.L., Sneck, M.E., Elderd, B.D., Iler, A.M., Inouye, D.W., Jacquemyn, H., et al. (2016). The effect of demographic correlations on the stochastic population dynamics of perennial plants. Ecol. Monogr. *86*, 480–494.

Cotto, O., Wessely, J., Georges, D., Klonner, G., Schmid, M., Dullinger, S., Thuiller, W., and Guillaume, F. (2017). A dynamic eco-evolutionary model predicts slow response of alpine plants to climate warming. Nat. Commun. *8*.

Coulson, T., Mace, G.M., Hudson, E., and Possingham, H.P. (2001). The use and abuse of population viability analysis. Trends Ecol. Evol. *16*, 219–221.

Crawley, M.J. (2012). The R book (John Wiley & Sons).

Crone, E.E., Menges, E.S., Ellis, M.M., Bell, T., Bierzychudek, P., Ehrlén, J., Kaye, T.N., Knight, T.M., Lesica, P., Morris, W.F., et al. (2011). How do plant ecologists use matrix population models? Ecol. Lett. *14*, 1–8.

Crone, E.E., Ellis, M.M., Morris, W.F., Stanley, A., Bell, T., Bierzychudek, P., Ehrlen, J., Kaye, T.N., Knight, T.M., Lesica, P., et al. (2013). Ability of matrix models to explain the past and predict the future of plant populations. Cons. Biol. *27*, 968–978.

Csergő, A.M., Salguero-Gómez, R., Broennimann, O., Coutts, S.R., Guisan, A., Angert, A.L., Welk, E., Stott, I., Enquist, B.J., McGill, B., et al. (2017). Less favourable climates constrain demographic strategies in plants. Ecol. Lett. *20*, 969–980.

Davison, R., Jacquemyn, H., Adriaens, D., Honnay, O., De Kroon, H., and Tuljapurkar, S. (2010). Demographic effects of extreme weather events on a short-lived calcareous grassland species: stochastic life table response experiments. J. Ecol. *98*, 255–267.

Doak, D.F., and Morris, W.F. (2010). Demographic compensation and tipping points in climate-induced range shifts. Nature *467*, 959–962.

Ducrocq, V. (2016). Climate change in the Mediterranean region. In The Mediterranean Region under Climate Change, (Paris: IRD Editions), p. 71.

Eckhart, V.M., Geber, M.A., Morris, W.F., Fabio, E.S., Tiffin, P., and Moeller, D.A. (2011). The geography of demography: Long-term demographic studies and species distribution models reveal a species border limited by adaptation. Am. Nat. *178*, S26–S43.

Ehrlén, J., Morris, W.F., von Euler, T., and Dahlgren, J.P. (2016). Advancing environmentally explicit structured population models of plants. J. Ecol. *104*, 292–305.

Engen, S., Bakke, Ø., and Islam, A. (1998). Demographic and Environmental Stochasticity-Concepts and Definitions. Biometrics 54, 840–846.

Engen, S., Lande, R., Sæther, B.-E., and Weimerskirch, H. (2005). Extinction in relation to demographic and environmental stochasticity in age-structured models. Math. Bio 195, 210–227.

Fant, J.B., Kramer, A., Sirkin, E., and Havens, K. (2013). Genetics of reintroduced populations of the narrowly endemic thistle, *Cirsium pitcher*i (Asteraceae). Botany *91*, 301–308.

Fieberg, J., and Ellner, S.P. (2001). Stochastic matrix models for conservation and management: a comparative review of methods. Ecol. Lett. *4*, 244–266.

Franklin, J., Serra-Diaz, J.M., Syphard, A.D., and Regan, H.M. (2017). Big data for forecasting the impacts of global change on plant communities. Glob. Ecol. Biogeogr. *26*, 6–17.

Franks, S.J., Weber, J.J., and Aitken, S.N. (2014). Evolutionary and plastic responses to climate change in terrestrial plant populations. Evol. Appl. *7*, 123–139.

Fréville, H., Colas, B., Ronfort, J., Riba, M., and Olivieri, I. (1998). Predicting endemism from population structure of a widespread species: case study in *Centaurea maculosa Lam.* (Asteraceae). Conserv. Biol. *12*, 1269–1278.

Fréville, H., Justy, F., and Olivieri, I. (2001). Comparative allozyme and microsatellite population structure in a narrow endemic plant species, *Centaurea corymbosa* Pourret (Asteraceae). Mol. Ecol. *10*, 879–889.

Fréville, H., Colas, B., Riba, M., Caswell, H., Mignot, A., Imbert, E., and Olivieri, I. (2004). Spatial and temporal demographic variability in the endemic plant species *Centaurea corymbosa* (Asteraceae). Ecology *85*, 694–703.

Fujiwara, M., and Caswell, H. (2001). Demography of the endangered North Atlantic right whale. Nature 414, 537–541.

Gao X., and Giorgi, F. (2008). Increased aridity in the Mediterranean region under greenhouse gas forcing estimated from high resolution simulations with a regional climate model. Glob. Plan. Change 62: 195-209.

García, M.B. (2003). Demographic viability of a relict population of the critically endangered plant Borderea chouardii. Conserv. Biol. *17*, 1672–1680.

García, M.B., Guzmán, D., and Goñi, D. (2002). An evaluation of the status of five threatened plant species in the Pyrenees. Biol. Conserv. *103*, 151–161.

Groom, M.J., Meffe, G.K., and Carroll, C.R. (2005). Principles of conservation biology (Sinauer Associates, Inc.).

Hardy, O.J., González-Martínez, S.C., Colas, B., Fréville, H., Mignot, A., and Olivieri, I. (2004). Fine-scale genetic structure and gene dispersal in *Centaurea corymbosa* (Asteraceae). II. Correlated paternity within and among sibships. Genetics *168*, 1601–1614.

Heller, N.E., and Zavaleta, E.S. (2009). Biodiversity management in the face of climate change: A review of 22 years of recommendations. Biol. Conserv. *142*, 14–32.

Hens, H., Pakanen, V.-M., Jäkäläniemi, A., Tuomi, J., and Kvist, L. (2017). Low population viability in small endangered orchid populations: Genetic variation, seedling recruitment and stochasticity. Biol. Cons. *210*, 174–183.

23

Huelber, K., Wessely, J., Gattringer, A., Moser, D., Kuttner, M., Essl, F., Leitner, M., Winkler, M., Ertl, S., Willner, W., et al. (2016). Uncertainty in predicting range dynamics of endemic alpine plants under climate warming. Glob. Change Biol. *22*, 2608–2619.

Hunter, C.M., Caswell, H., Runge, M.C., Regehr, E.V., Amstrup, S.C., and Stirling, I. (2010). Climate change threatens polar bear populations: a stochastic demographic analysis. Ecology *91*, 2883–2897.

Imbert, E. (2006). Dispersal by ants in *Centaurea corymbosa* (Asteraceae): What is the elaiosome for? P. Spec. Biol. *21*, 109–117.

Imbert, E., Youssef, S., Carbonell, D., and Baumel, A. (2012). Do endemic species always have a low competitive ability? A test for two Mediterranean plant species under controlled conditions. J. P. Ecol. *5*, 305–312.

IPCC (2007). Climate Change 2007 - The physical science basis: Working group I contribution to the fourth assessment report of the intergovernmental panel on climate change (United Kingdom and New York, NY, USA: Cambridge University Press).

Isik, K. (2011). Rare and endemic species: why are they prone to extinction? Turk. J. Bot. *35*, 411–417.

Jacob, D., Petersen, J., Eggert, B., Alias, A., Christensen, O.B., Bouwer, L.M., Braun, A., Colette, A., Deque, M., Georgievski, G., et al. (2014). EURO-CORDEX: new high-resolution climate change projections for European impact research. Reg. Environ. Change *14*, 563–578.

Jeppsson, T., and Forslund, P. (2012). Can Life History Predict the Effect of Demographic Stochasticity on Extinction Risk? Am. Nat. 179, 706–720.

Jolls, C.L., Marik, J.E., Hamzé, S.I., and Havens, K. (2015). Population viability analysis and the effects of light availability and litter on populations of Cirsium pitcheri, a rare, monocarpic perennial of Great Lakes shorelines. Biol. Cons. *187*, 82–90.

Kaye, T.N., and Pyke, D.A. (2003). The effect of stochastic technique on estimates of population viability from transition matrix models. Ecol. *84*, 1464–1476.

Kirchner, F., Luijten, S.H., Imbert, E., Riba, M., Mayol, M., González-Martínez, S.C., Mignot, A., and Colas, B. (2005). Effects of local density on insect visitation and fertilization success in the narrow-endemic *Centaurea corymbosa* (Asteraceae). Oikos *111*, 130–142.

Kirchner, F., Robert, A., and Colas, B. (2006). Modelling the dynamics of introduced populations in the narrow-endemic *Centaurea corymbosa*: a demo-genetic integration. J. Appl. Ecol. *43*, 1011–1021.

Kiviniemi, K., and Löfgren, A. (2009). Spatial (a) synchrony in population fluctuations of five plant species in fragmented habitats. Bas. Appl. Ecol. *10*, 70–78.

Lande, R. (1993). Risks of Population Extinction from Demographic and Environmental Stochasticity and Random Catastrophes. Amer. Nat. 142, 911–927.

Lande, R., Engen, S., and Saether, B.-E. (2003). Stochastic population dynamics in ecology and conservation (Oxford ; New York: Oxford University Press).

Larson, D.W., Matthes, U., Gerrath, J.A., Larson, N.W.K., Gerrath, J.M., Nekola, J.C., Walker, G.L., Porembski, S., and Charlton, A. (2000). Evidence for the widespread occurrence of ancient forests on cliffs. J. Biogeogr. *27*, 319–331.

Lavergne, S., Thompson, J.D., Garnier, E., and Debussche, M. (2004). The biology and ecology of narrow endemic and widespread plants: a comparative study of trait variation in 20 congeneric pairs. Oikos *107*, 505–518.

Lavergne, S., Thuiller, W., Molina, J., and Debussche, M. (2005). Environmental and human factors influencing rare plant local occurrence, extinction and persistence: a 115-year study in the Mediterranean region. J. Biogeogr. *32*, 799–811.

Lawson, C.R., Vindenes, Y., Bailey, L., and van de Pol, M. (2015). Environmental variation and population responses to global change. Ecol. Lett. *18*, 724–736.

Lennartsson, T., and Oostermeijer, J.G.B. (2001). Demographic variation and population viability in Gentianella campestris: effects of grassland management and environmental stochasticity. J. Ecol. *89*, 451–463.

Lynch, M., Conery, J., and Burger, R. (1995). Mutation Accumulation and the Extinction of Small Populations. Am. Nat. *146*, 489–518.

Malcolm, J.R., Liu, C.R., Neilson, R.P., Hansen, L., and Hannah, L. (2006). Global warming and extinctions of endemic species from biodiversity hotspots. Cons. Biol. *20*, 538–548.

Manders, P.T., and Smith, R.E. (1992). Effects of watering regime on growth and competitive ability of nursery-grown Cape fynbos and forest plants. South Afr. J. Bot. *58*, 188–194.

Marrero-Gómez, M.V., Oostermeijer, J.G.B., Carqué-Álamo, E., and Bañares-Baudet, Á. (2007). Population viability of the narrow endemic *Helianthemum juliae* (Cistaceae) in relation to climate variability. Biol. Cons. *136*, 552–562.

Matesanz, S., Escudero, A., and Valladares, F. (2009). Impact of three global change drivers on a Mediterranean shrub. Ecology *90*, 2609–2621.

McDowell, N., Pockman, W.T., Allen, C.D., Breshears, D.D., Cobb, N., Kolb, T., Plaut, J., Sperry, J., West, A., Williams, D.G., et al. (2008). Mechanisms of plant survival and mortality during drought: why do some plants survive while others succumb to drought? New Phyt. *178*, 719–739.

Meer, S. van der, Jacquemyn, H., Carey, P.D., and Jongejans, E. (2016). Recent range expansion of a terrestrial orchid corresponds with climate-driven variation in its population dynamics. Oecologia *181*, 435–448.

Meisner, M.H., Harmon, J.P., and Ives, A.R. (2014). Temperature effects on long-term population dynamics in a parasitoid-host system. Ecol. Monogr. *84*, 457–476.

Melbourne, B.A., and Hastings, A. (2008). Extinction risk depends strongly on factors contributing to stochasticity. Nature *454*, 100–103.

Menges, E. (2008). TURNER REVIEW No. 16. Restoration demography and genetics of plants: when is a translocation successful? Aust. J. Bot. -*56*.

Menges, E.S. (2000). Population viability analyses in plants: challenges and opportunities. Trends Ecol. Evol. *15*, 51–56.

Metcalf, J.C., Rose, K.E., and Rees, M. (2003). Evolutionary demography of monocarpic perennials. Tren. Ecol. Evol. *18*, 471–480.

26

Morris, W.F., Pfister, C.A., Tuljapurkar, S., Haridas, C.V., Boggs, C.L., Boyce, M.S., Bruna, E.M., Church, D.R., Coulson, T., Doak, D.F., et al. (2008). Longevity can buffer plant and animal populations against changing climatic variability. Ecology *89*, 19–25.

Morris, W.F., and Doak, D.F. (2002). Quantitative Conservation Biology: Theory and Practice of Population Viability Analysis (Sunderland, Mass: OUP USA).

Nakagawa, S., and Schielzeth, H. (2013). A general and simple method for obtaining R2 from generalized linear mixed-effects models. Meth. Ecol. Evol. *4*, 133–142.

Nicolè, F., Dahlgren, J.P., Vivat, A., Till-Bottraud, I., and Ehrlén, J. (2011). Interdependent effects of habitat quality and climate on population growth of an endangered plant. J. Ecol. *99*, 1211–1218.

Noel, F., Maurice, S., Mignot, A., Glemin, S., Carbonell, D., Justy, F., Guyot, I., Olivieri, I., and Petit, C. (2010). Interaction of climate, demography and genetics: a ten-year study of *Brassica insularis*, a narrow endemic Mediterranean species. Cons. Genet. *11*, 509–526.

Olivieri, I., Tonnabel, J., Ronce, O., and Mignot, A. (2016). Why evolution matters for species conservation: perspectives from three case studies of plant metapopulations. Evol. Appl. *9*, 196–211.

Peñuelas, J., Gordon, C., Llorens, L., Nielsen, T., Tietema, A., Beier, C., Bruna, P., Emmett, B., Estiarte, M., and Gorissen, A. (2004). Nonintrusive field experiments show different plant responses to warming and drought among sites, seasons, and species in a north–south european gradient. Ecosystems *7*, 598–612.

Ramula, S., Puhakainen, L., Suhonen, J., and Vallius, E. (2008). Management actions are required to improve the viability of the rare grassland herb Carlina biebersteinii. Nor. J. Bot. *26*, 83–90.

Picó, F.X., and Riba, M. (2002). Regional-scale demography of *Ramonda myconi*: Remnant population dynamics in a preglacial relict species. Plant Ecol. *161*, 1–13.

Riba, M., Picó, F. x., and Mayol, M. (2002). Effects of regional climate and small-scale habitat quality on performance in the relict species *Ramonda myconi*. J. Veg. Sci. *13*, 259–268.

Riba, M., Mignot, A., Fréville, H., Colas, B., Imbert, E., Vile, D., Virevaire, M., and Olivieri, I. (2005). Variation in dispersal traits in a narrow-endemic plant species, *Centaurea corymbosa* Pourret. (Asteraceae). Evol. Ecol. *19*, 241–254.

Ruffault, J., Martin-StPaul, N.K., Duffet, C., Goge, F., and Mouillot, F. (2014). Projecting future drought in Mediterranean forests: bias correction of climate models matters! Theor. Appl. Climatol. *117*, 113–122.

Ruiz-Sinoga, J.D., Garcia-Marin, R., Gabarron-Galeote, M.A., and Martinez-Murillo, J.F. (2012). Analysis of dry periods along a pluviometric gradient in Mediterranean southern Spain. Int. J. Climatol. *32*, 1558–1571.

Salguero-Gomez, R., Siewert, W., Casper, B.B., and Tielboerger, K. (2012). A demographic approach to study effects of climate change in desert plants. Philos. Trans. R. Soc. B-Biol. Sci. *367*, 3100–3114.

Selwood, K.E., McGeoch, M.A., and Mac Nally, R. (2015). The effects of climate change and land-use change on demographic rates and population viability. Biol. Rev. *90*, 837–853.

Semenov, V.A., and Bengtsson, L. (2002). Secular trends in daily precipitation characteristics: greenhouse gas simulation with a coupled AOGCM. Clim. Dyn. *19*, 123–140.

Shriver, R.K. (2016). Quantifying how short-term environmental variation leads to long-term demographic responses to climate change. J. Ecol. *104*, 65–78.

Shryock, D.F., Esque, T.C., and Hughes, L. (2014). Population viability of pediocactus bradyi (cactaceae) in a changing climate. Am. J. Bot. *101*, 1944–1953.

Silva, J.L., Mejías, J.A., and García, M.B. (2015). Demographic vulnerability in cliff-dwelling Sonchus species endemic to the western Mediterranean. Basic Appl. Ecol. *16*, 316–324.

Stubben, C., and Milligan, B. (2007). Estimating and analyzing demographic models using the popbio package in R. J. Stat. Softw. *22*, 1–23.

Thomann, M., Imbert, E., Devaux, C., and Cheptou, P.-O. (2013). Flowering plants under global pollinator decline. Tren. P. Sci. *18*, 353–359.

Thomas, J.A., Telfer, M.G., Roy, D.B., Preston, C.D., Greenwood, J.J.D., Asher, J., Fox, R., Clarke, R.T., and Lawton, J.H. (2004). Comparative losses of British butterflies, birds, and plants and the global extinction crisis. Science *303*, 1879–1881.

Thompson, J.D., Lavergne, S., Affre, L., Gaudeul, M., and Debussche, M. (2005). Ecological differentiation of Mediterranean endemic plants. Taxon *54*, 967–976.

Thuiller, W., Lavorel, S., and Araújo, M.B. (2005). Niche properties and geographical extent as predictors of species sensitivity to climate change. Glob. Ecol. Biogeogr. *14*, 347–357.

Treurnicht, M., Pagel, J., Esler, K.J., Schutte-Vlok, A., Nottebrock, H., Kraaij, T., Rebelo, A.G., and Schurr, F.M. (2016). Environmental drivers of demographic variation across the global geographical range of 26 plant species. J. Ecol. *104*, 331–342.

Tuffa, S., and Treydte, A.C. (2017). Modeling Boran cattle populations under climate change and varying carrying capacity. Ecol. Model. *352*, 113–127.

Ulrey, C., Quintana-Ascencio, P.F., Kauffman, G., Smith, A.B., and Menges, E.S. (2016). Life at the top: Long-term demography, microclimatic refugia, and responses to climate change for a high-elevation southern Appalachian endemic plant. Biol. Cons. *200*, 80–92.

Whitlock, M., and Schluter, D. (2009). The analysis of biological data (Roberts and Company Publishers).

Wiens, J.J. (2016). Climate-Related Local Extinctions Are Already Widespread among Plant and Animal Species. PLOS Biol. *14*, e2001104.

Williams, J.L., Jacquemyn, H., Ochocki, B.M., Brys, R., and Miller, T.E.X. (2015). Life-history evolution under climate change and its influence on the population dynamics of a long-lived plant. J. Ecol. *103*, 798–808.

Yordanov, I., Velikova, V., and Tsonev, T. (2000). Plant responses to drought, acclimation, and stress tolerance. Photosynthetica *38*, 171–186.

Zeigler, S. (2013). Predicting responses to climate change requires all life-history stages. J. Anim. Ecol. *82*, 3–5.

570

Tables

Table 1: Demographic characteristics of each of the six populations of *Centaurea corymbosa*, and the pooled population after pooling data across populations: number of individual life-histories recorded over 22 years (see also Appendix A1), number of surviving plants older than 1 year, mean life-time of individuals that reached the rosette stage, mean age at flowering, geometric mean of asymptotic growth rates (λ_a) over 22 years, minimum and maximum of λ_a, stochastic growth rate (λ_s) when including both demographic and environmental stochasticity (uniform frequency, see text) with the confidence intervals (2.5[th] and 97.5[th] percentiles of the simulated distributions) and the rounded mean of total numbers of flowering plants (Nb.FP) recorded by the exhaustive count over the 22 years (see appendix A2). Populations are ranked by decreasing order of total number of flowering plants.

Population	Nb. individuals	Nb. one year plants	Mean longevity of the rosettes (years)	Mean age at flowering (years)	Mean λ_a	[$\lambda_a$min, $\lambda_a$max]	λ_s	$CI(\lambda_s)$	Nb.FP
Pooled pop.	6112	1579	3.5	5.0	0.880	[0.432, 1.815]	0.881	[0.877, 0.889]	478
Enferret2	1712	286	3.3	4.5	0.749	[0.240, 1.585]	0.836	[0.829, 0.851]	173
Enferret1	1165	324	3.6	5.1	0.836	[0.425, 2.325]	0.824	[0.819, 0.837]	147
Auzils	1175	415	3.5	5.7	0.783	[0.331, 1.391]	0.792	[0.786, 0.807]	81
Portes	1064	268	3.7	6.2	0.819	[0.364, 1.610]	0.824	[0.818, 0.842]	34
Peyral	540	192	3.2	4.7	0.710	[0.00[(a)], 1.264]	0.804	[0.799, 0.827]	28
Cruzade	456	94	3.4	4.2	0.720	[0.00[(a)], 1.444]	0.742	[0.732, 0.770]	13

(a) The null values of asymptotic growth rates corresponded to pair-of-years with no flowering plant within plots and null values for rosette survival s_2.

580 **Table 2:** Summary of GLMs explaining the effect of two climatic variables (averaged over three-month periods) on lower-level vital rates. Only
581 climatic variables affecting population growth rate were included in the GLMs. From the best model explaining a given lower-level vital rate, we
582 report the estimated coefficient (β) and its significance (*t-test*) after scaling the climatic variables. 'ns' indicates that the variable tested was not
583 significant in the model, based on a forward stepwise selection approach (see text and appendix E.3 for details).

	Daily mean temperature				No. wet days			
	Summer [Jun-Aug]	Fall [Sep-Nov]	Winter [Dec-Fev]	Spring [Mar-May]	Summer [Jun-Aug]	Fall [Sep-Nov]	Winter [Dec-Fev]	Spring [Mar-May]
Fecundity term $log(f+1)$	-0.28 **	-0.22 *	ns	ns	ns	ns	ns	ns
Survival of just emerged seedling s_0	-0.17 ***	-0.08*	ns	ns	ns	0.24 ***	0.14 ***	ns
Seedling survival s_1	-0.28 ***	-0.12$^+$	ns	ns	0.34 ***	0.04 $^+$	ns	ns
Rosette survival s_2	-0.45 ***	ns	ns	ns	ns	ns	ns	ns
Flowering probability of rosette α_2	-0.23 ***	ns	ns	ns	ns	0.19 *	ns	ns

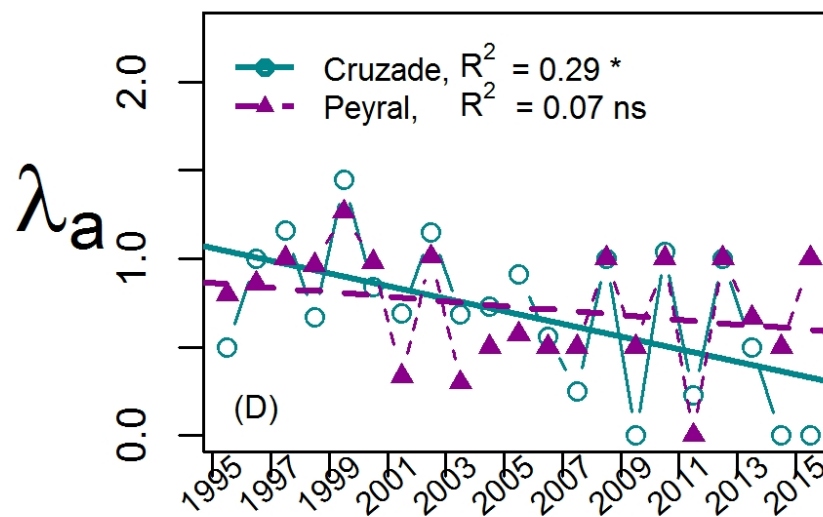584 $^+$P <0.08, *P < 0.05, **P < 0.01, ***P < 0.001.
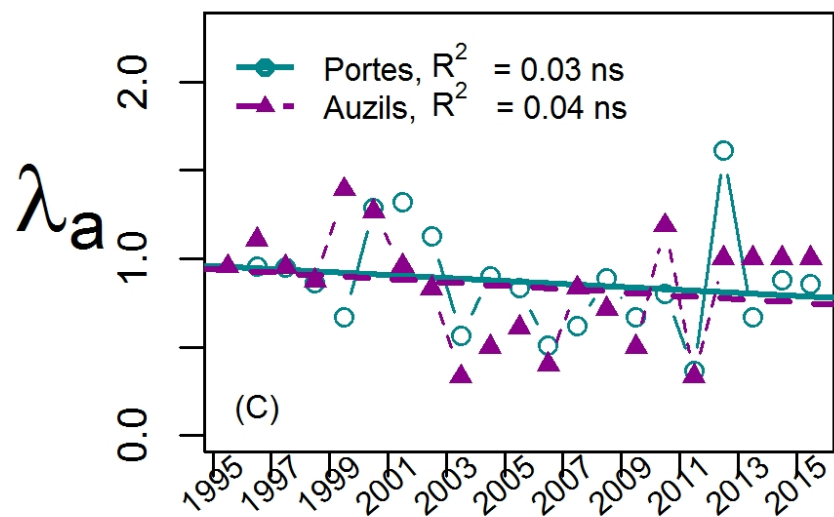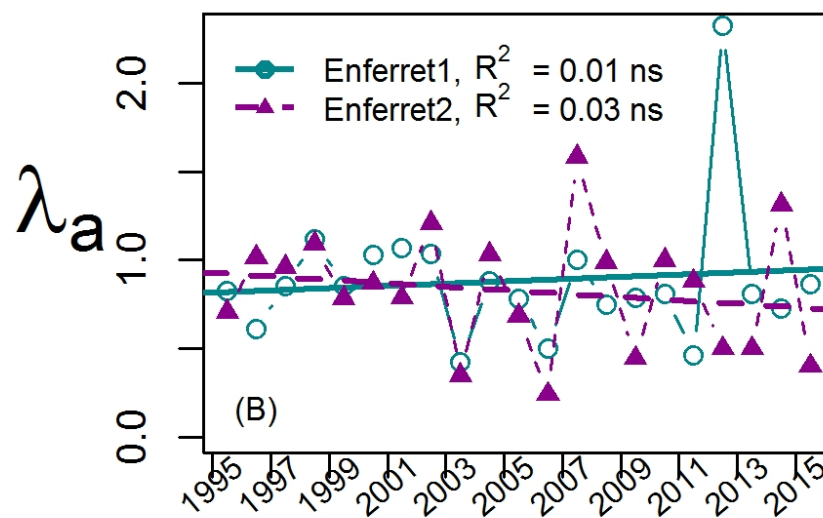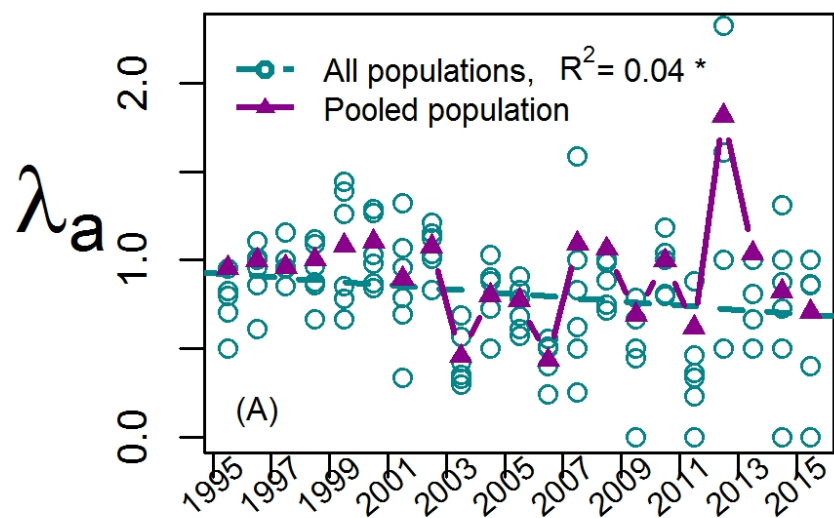
2

Figure legends

586 **Figure 1:** Climatic variation observed in the Massif de la Clape between 1995 and 2016. Climatic
587 variables were calculated per pair-of-years from June(t) to May($t+1$). The solid line represents the
588 average daily mean temperature (C°), and the dashed line represents the number of wet days.
589 Values in the vertical bars indicate the cumulative precipitation per pair-of-years. Year on the x-axis
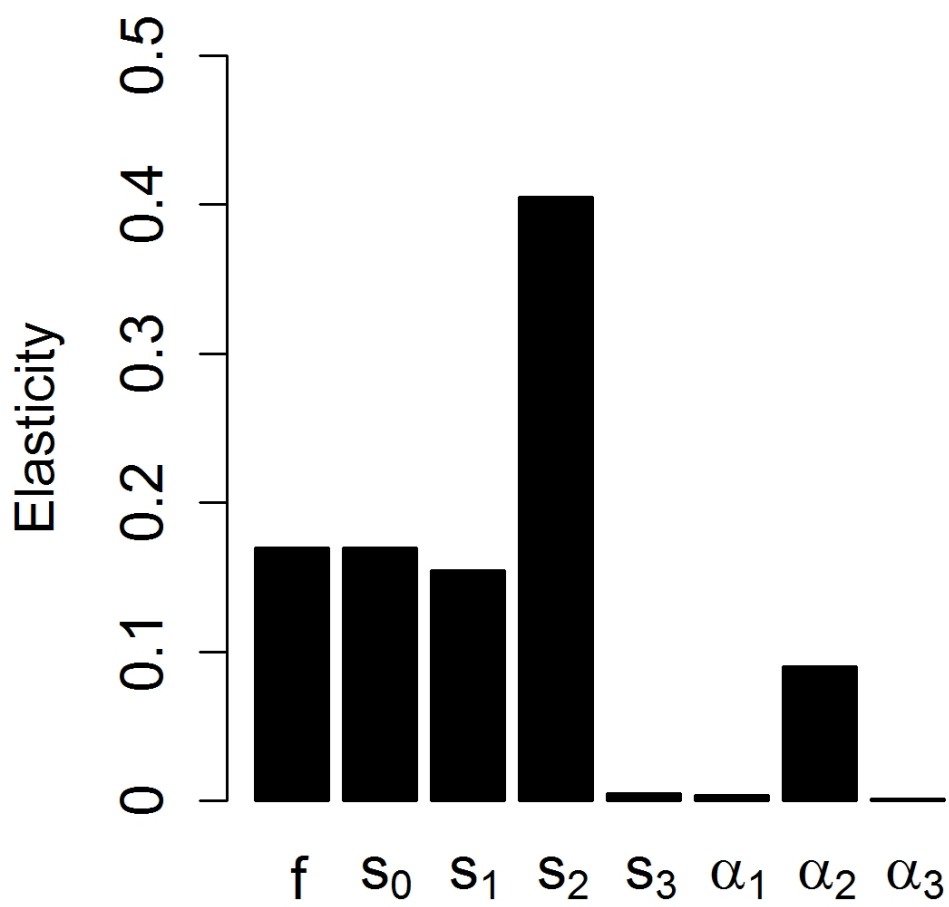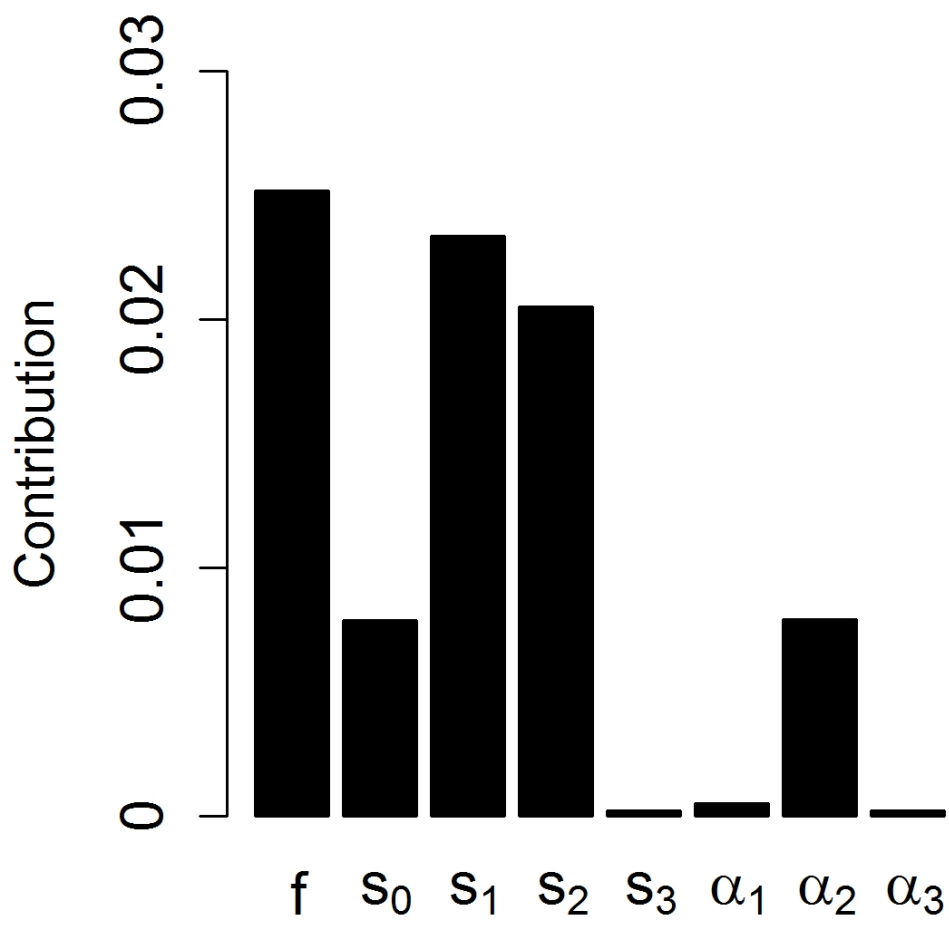590 corresponds to June(t). Data were obtained from INRA Pech Rouge.

591 **Figure 2:** Asymptotic growth rates (λ_a) per pair-of-years. Panel A represents yearly λ_a values
592 (circles) with their trend over years (dashed line) calculated from 125 matrices. The solid line
593 represents the values of λ_a (triangles) pooling individuals in a single population. Panels B, C and D
594 represent the trend in λ_a over years for the largest populations (E2 and E1), the medium size
595 populations (Au and Po) and the smallest ones (Pe and Cr). R^2 corresponds to the r-squared value
596 obtained from the linear regression and "ns" indicates that the slope was not significantly different
597 from 0. Year on the x-axis corresponds to June (t).

598 **Figure 3:** Contribution of lower-level vital rates to the variance of λ_a observed among years, and
599 elasticity of growth rates to these vital rates calculated on the arithmetic mean matrix calculated
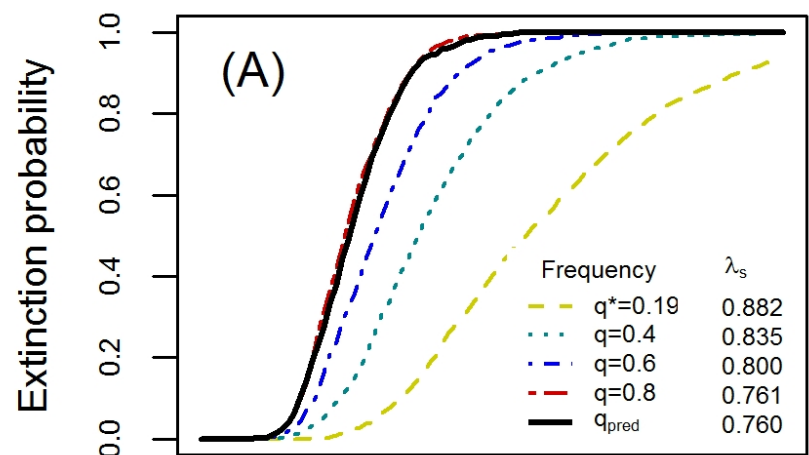600 over 21 pair-of-years matrices.

601 **Figure 4**: Predicted consequences of the warm and dry scenarios on the viability of populations
602 using two different initial population sizes representing the largest (Enferret2) and the smallest
603 (Cruzade) populations when incorporating both demographic and environmental stochasticity (see
604 text for details). Panels (A) and (C) represent the warm scenario for the largest population size ($N_0 =$
605 {685 796 118}, Enferret2), and the smallest one ($N_0 =$ {41 47 7}, Cruzade). Panels (B) and (D)
606 represent the dry scenario for Enferret2 and Cruzade, respectively. The warm scenario consisted of
607 an increase in the frequency of years with extremely high temperatures (4 extreme years out of 21:
608 2006-2007, 2013-2014, 2014-2015), and the dry scenario an increase in the frequency of years with
609 an extremely low number of wet days (3 extreme years out of 21: 2001-2002, 2006-2007 and 2010-
610 2011). 'q' indicates the frequency of extreme years with q* the observed frequency over the 22-year
611 of our demographic survey and q_{pred} the frequency predicted by the RCP4.5 climatic model for the
612 warm and dry scenarios (q_{pred} are 0.78 and 0.15, respectively, see text). The initial population size
613 was estimated as the stable stage distribution predicted by the mean matrix over years after pooling
614 data across populations, using the mean total number of flowering plants recorded from 2010 to
615 2016 in Enferret2 and Cruzade, respectively.

3

Figure showing extinction probability over time for Warm scenario and Dry scenario.

Warm scenario

(A)

Frequency	λ_s
q*=0.19	0.882
q=0.4	0.835
q=0.6	0.800
q=0.8	0.761
q_{pred}	0.760

(C)

Frequency	λ_s
q*=0.19	0.879
q=0.4	0.839
q=0.6	0.805
q=0.8	0.765
q_{pred}	0.771

Dry scenario

(B)

Frequency	λ_s
q*=0.14	0.882
q=0.4	0.872
q=0.6	0.865
q=0.8	0.855
q_{pred}	0.883

(D)

Frequency	λ_s
q*=0.14	0.879
q=0.4	0.866
q=0.6	0.855
q=0.8	0.851
q_{pred}	0.874

N0 (Enferret2)

N0 (Cruzade)

Extinction probability

Time (years)
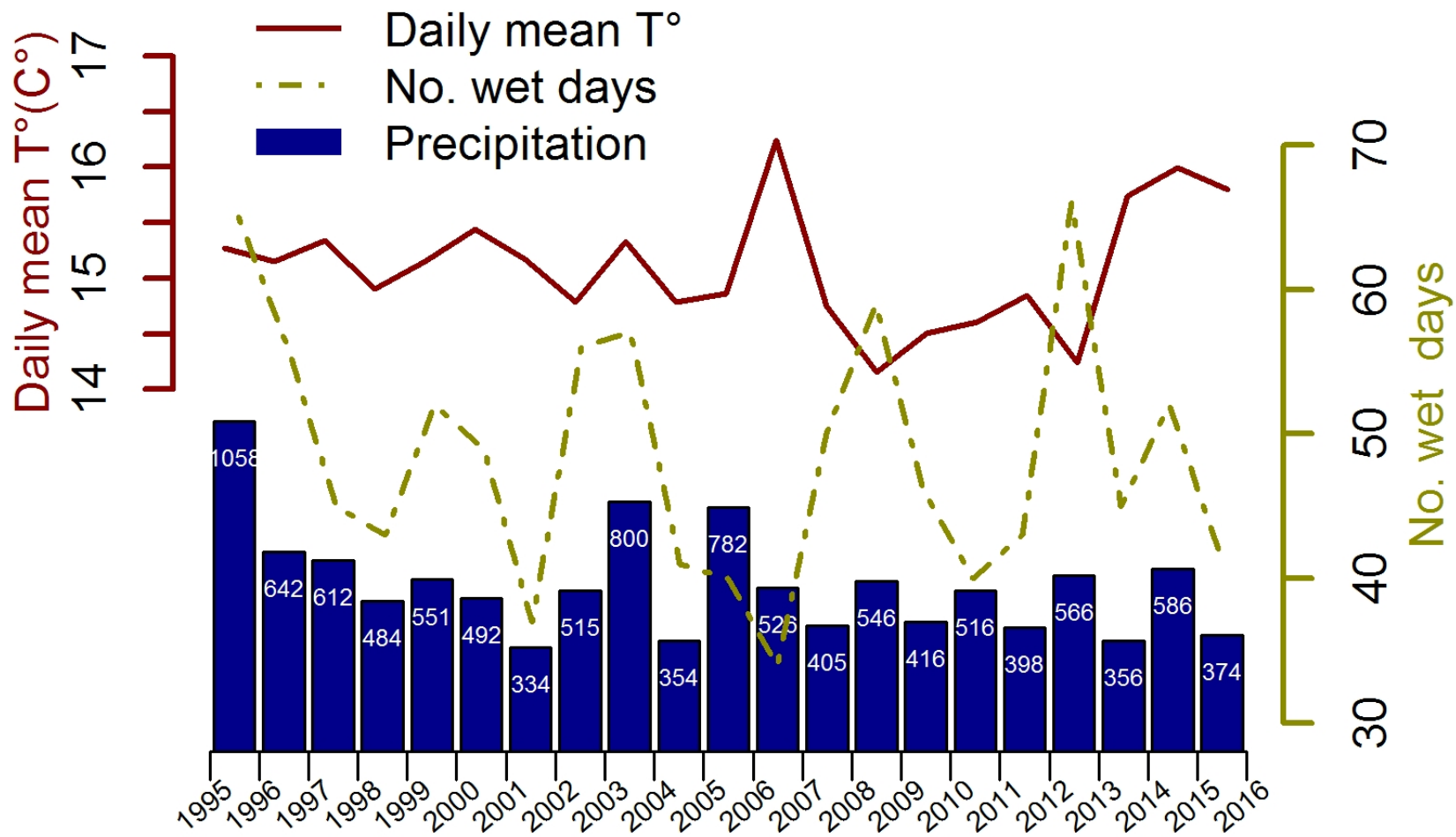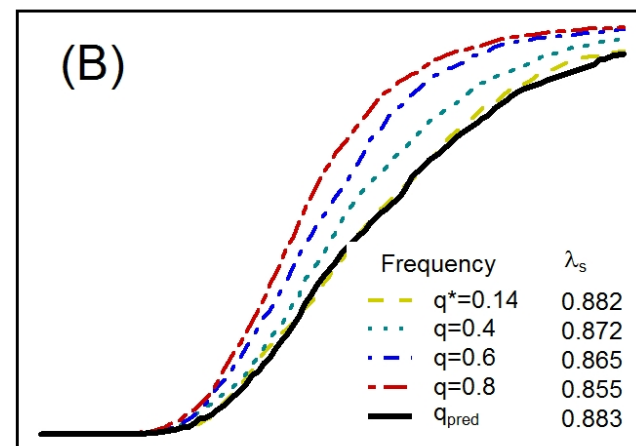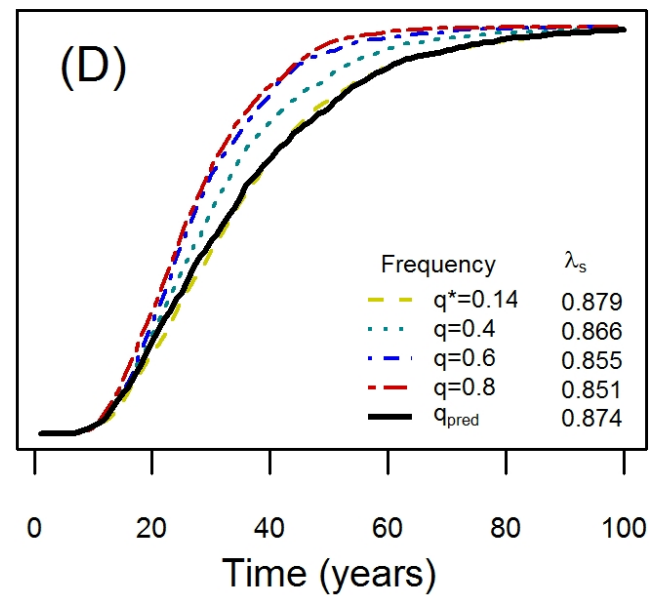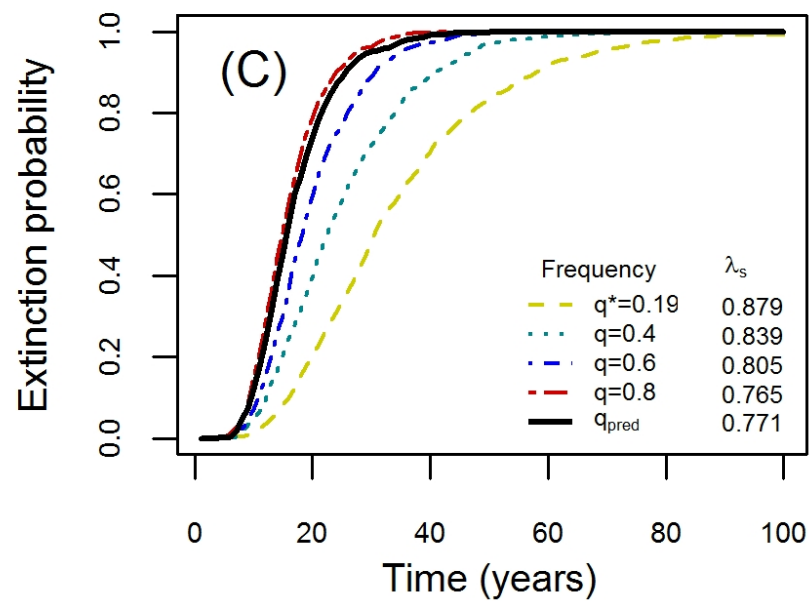
Appendices:

Appendix A1: Number of individuals recorded within the 41 permanent plots over the 22-year period. Number of new seedlings represents all new plants recorded in the permanent plots every 3 months during year t to $t+1$, out of which some did not survive until June $t+1$ with a probability $1-s_0$, and thus did not reach the seedling stage. The number of individuals recorded in June (t) in each life-stage of the life-cycle used to construct population projection models, is given for: Seedling, the one-year plants that survive until June (t), Rosette, vegetative plants older than one year, and Flowering plants that represent reproductive plants. The total number of individuals per year did not include the new seedlings. The total individual life-histories (6112) corresponds to the sum of number of new seedlings (5779) and number of rosettes and flowering plants at the first census (315+18).

| Year	New seedlings	Seedling stage	Rosette stage	Flowering plant stage	Total
1994	NA	NA	315	18	333
1995	467	234	161	35	430
1996	258	145	184	48	377
1997	608	181	160	48	389
1998	427	165	195	28	388
1999	349	204	178	37	419
2000	284	164	218	41	423
2001	1097	475	204	30	709
2002	466	356	250	17	623
2003	167	115	357	30	502
2004	299	197	144	12	353
2005	73	45	137	17	199
2006	262	30	97	22	149
2007	72	42	40	9	91
2008	182	47	45	9	101
2009	368	102	43	6	151
2010	67	29	36	3	68
2011	29	15	44	3	62
2012	50	8	20	6	34
2013	116	93	19	7	119
2014	89	45	41	4	90
2015	31	10	48	5	63
2016	18	9	35	2	46
Total	5779	2711	2971	437	

Appendix A2: Total number of flowering plants per year recorded by the exhaustive count per population. The dashed line corresponds to the trend of the number of flowering plants over time (β = -2.21, p = 0.02). The growth rate calculated from the number of flowering plants was equal to 0.92.
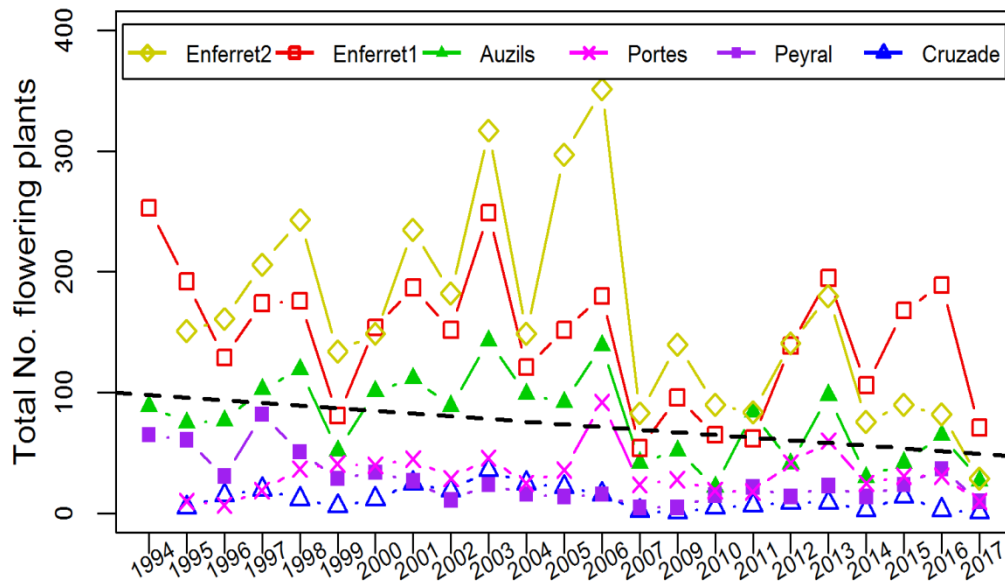
Appendix B: Projections matrices per population. The fecundity term fs_0 was estimated as the geometric mean of fs_0 obtained per pair-of-years, other parameters are obtained by pooling data over years.

Population	a_{13} fs_0	a_{21} $s_1 (1-\alpha_1)$	a_{22} $s_2 (1-\alpha_2)$	a_{23} $s_3 (1-\alpha_3)$	a_{31} $s_1 \alpha_1$	a_{32} $s_2 \alpha_2$	a_{33} $s_3 \alpha_3$
Pooled pop.	5.104	0.351	0.586	0.024	0.011	0.120	0.038
Enferret2	4.267	0.345	0.509	0.029	0.029	0.165	0.029
Enferret1	3.834	0.347	0.595	0.000	0.009	0.119	0.035
Auzils	4.549	0.379	0.598	0.026	0.000	0.094	0.026
Portes	4.283	0.294	0.640	0.017	0.011	0.113	0.017
Peyral	3.601	0.404	0.573	0.067	0.000	0.108	0.067
Cruzade	2.819	0.361	0.593	0.020	0.016	0.174	0.082

Appendix C: Distribution of the standard deviation of asymptotic growth rates under the null hypothesis of: (A) no difference among years and (B) no difference among populations. The x-axis represents the standard deviation of λ_a calculated (A) over the 21 year values, (B) over the 6 population values. The y-axis represents the number of observations. The dashed vertical lines indicate the observed value. Randomization tests were based on 2000 permutations.
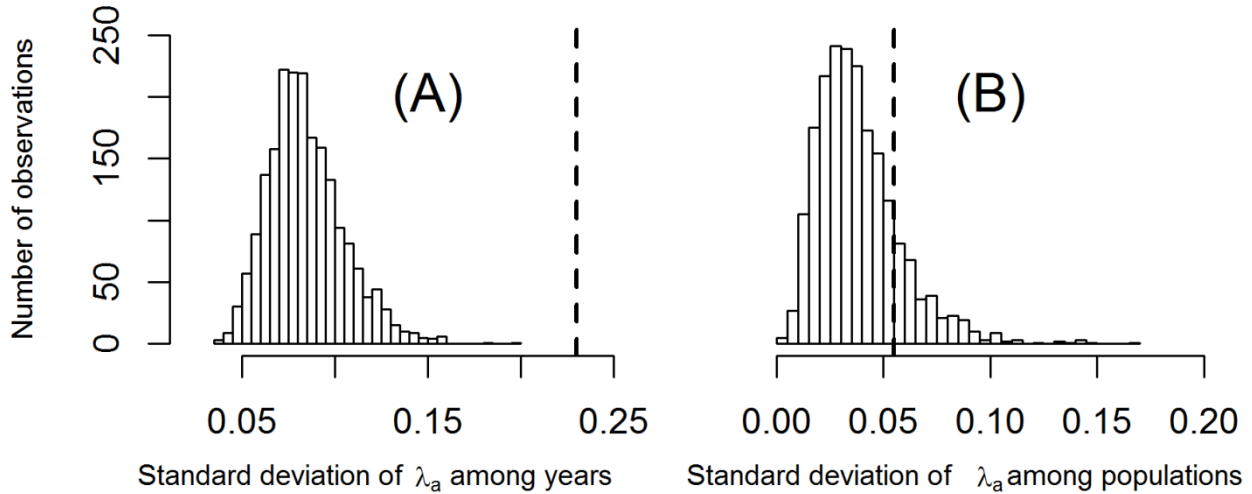
Appendix D: Arithmetic mean and coefficient of variation of lower-level vital rates over years after pooling data over populations, sensitivity and elasticity of growth rates to these vital rates calculated at the arithmetic mean matrix over 21 matrices, and contributions of lower-level vital rates to the variation of growth rates among years.

	f	s_0	s_1	s_2	s_3	α_1	α_2	α_3
Mean	13.235	0.484	0.363	0.732	0.059	0.016	0.181	0.217
CV	0.644	0.395	0.505	0.184	1.046	2.598	0.386	1.352
Sensitivity	0.017	0.457	0.55	0.721	0.117	0.31	0.648	0.008
Elasticity	0.170	0.170	0.155	0.405	0.005	0.004	0.090	0.001
Contribution	0.025	0.008	0.023	0.021	<0.001	<0.001	0.008	<0.001

Appendix E.1: Single-variable log-linear models showing the relationship between asymptotic growth rates and each climatic variable. R^2 corresponds to the coefficient of determination for the tested model.

Climatic variable in year t	R^2	Estimate	p-value
Daily mean T°	0.31	-0.320	**0.011**
Daily maximal T°	0.30	-0.250	**0.009**
Precipitation	0.01	-0.001	0.672
No. days with T°>25	0.18	-0.013	0.052
No. freezing days	0.03	0.008	0.451
No. wet days	0.46	0.021	**0.001**
No. days with precip.>20mm	0.04	-0.021	0.381
Climatic variables in year $t-1$			
Daily mean T°	0.003	0.031	0.251
Daily maximal T°	0.006	0.032	0.233
Precipitation	0.058	-0.001	0.452
No. days with T°>25	0.005	-0.002	0.253
No. freezing days	0.001	0.001	0.360
No. wet days	0.012	-0.004	0.250
No. days with precip.>20mm	0.010	-0.009	0.141
Quadratic effect			
Daily mean T°	0.30	-0.011	**0.010**
Daily maximal T°	0.30	-0.006	**0.009**
Precipitation	0.01	0.000	0.631
No. days with T°>25	0.18	-0.001	0.052
No. freezing days	0.02	0.000	0.540
No. wet days	0.43	0.003	**0.002**
No. days with precip.>20mm	0.04	-0.001	0.411

Appendix E.2: Selection models for assessing the relevance of climatic variables to explain variations in asymptotic growth rates based on a forward stepwise selection approach. The significance of each added variable in the model was tested using an analysis of deviance. The null model included only the intercept.

Model	Compared models	p-value
M0: Null model		
M1: No. wet days	M0, M1	**0.001**
M2: No. wet days + (No. wet days)^2	M1, M2	0.311
M3: No. wet days + Daily mean T°	M1, M3	**0.031**
M4: No. wet days + Daily mean T°+ (Daily mean T°)^2	M3, M4	0.292
M5: No. wet days + Daily mean T°+ Daily maximal T°	M3, M5	0.890
M6: No. wet days + Daily mean T°+ (Daily maximal T°)^2	M3, M6	0.843

Appendix E.3: Selection models for assessing the relevance of climatic variables to explain variations in lower-level vital rates based on a forward stepwise selection approach. P-values correspond to the F-test for the log-linear models and to Chi-test for the generalized linear models with binomial error. The null model included only the intercept. We denoted the number of days with Precipitation > 1mm by **"P"** and the mean daily temperature by **"T"**. The seasons are denoted by **1, 2, 3 and 4** to indicate **summer, fall, winter and spring,** respectively (see the main text and Table 2)

Lower-level vital rate	Model	Compared models	p-value
log(f+1)	M0: Null model		
	M1: T1	M0, M1	**0.012**
	M2: T1+T2	M1, M2	**0.031**
	M3: T1+T2+T3	M2, M3	0.165
	M4: T1+T2+T4	M2, M4	0.583
	M5: T1+T2+P1	M2, M5	0.794
	M6: T1+T2+P2	M2, M6	0.222
	M7: T1+T2+P3	M2, M7	0.806
	M8: T1+T2+P4	M2, M8	0.236
	Selected model: log (*f+1*) ~ T1+T2		
S_0	M0: Null model		
	M1: P2	M0, M1	**<0.001**
	M2: P2+P3	M1, M2	**<0.001**
	M3: P2+P3+T2	M2, M3	**0.006**
	M4: P2+P3+T2+T1	M3, M4	**<0.001**
	M5: P2+P3+T2+T1+P1	M4, M5	0.082
	M6: P2+P3+T2+T1+T3	M4, M6	0.087
	M7: P2+P3+T2+T1 +T4	M4, M7	0.120
	M8: P2+P3+T2+T1 +P4	M4, M8	0.091
	Selected model: S_0 ~ T1+T2+ P2+P3		
S_1	M0: Null model		
	M1: T1	M0, M1	**<0.001**
	M2: T1+P1	M1, M2	**<0.001**
	M3: T1+P1+P2	M2, M3	**0.002**
	M4: T1+P1+P2+T4	M3, M4	0.974

	M5: T1+P1+P2+P3	M3, M5	0.352
	M6: T1+P1+P2+P4	M3, M6	0.072
	M7: T1+P1+P2+T3	M3, M7	0.316
	M8: T1+P1+P2+T2	M3, M8	**0.030**
	Selected model: $S_1 \sim$ T1 +T2+ P1+ P2		
	M0: Null model		
	M1: T1	M0, M1	**<0.001**
	M2: T1 + P1	M1, M2	0.692
	M3: T1+P2	M1, M3	0.115
S₂	M4: T1+P3	M1, M4	0.174
	M5: T1+ P4	M1, M5	0.092
	M6: T1+ T2	M1, M6	0.163
	M7: T1+T3	M1, M7	0.662
	M8: T1+T4	M1, M8	0.365
	Selected model: $S_2 \sim$ T1		
	M0: Null model		
	M1: T1	M0, M1	**0.005**
	M2: T1+ T4	M1, M2	0.122
	M3: T1+P1	M1, M3	0.251
α₂	M4: T1+P4	M1, M4	0.071
	M5: T1+P2	M1, M5	**0.020**
	M6: T1+P2+P3	M5, M6	0.415
	M7:T1+P2+T2	M5, M7	0.868
	M8:T1+P2+T3	M5, M8	0.976
	Selected model: $\alpha_2 \sim$ T1+P2		

Appendix F: Relative effect of demographic stochasticity and environmental stochasticity on the viability of *C. corymbosa* populations. Simulations were performed either by incorporating only environmental stochasticity through whole matrix selection (see text), or both environmental stochasticity and demographic stochasticity introduced through multinomial sampling of the stable stage distribution (see text). Projections were simulated using 1000 stochastic iterations, each iteration representing a trajectory of population size over 100 years. The initial population size, $N_0 = \{2148, 2497, 370\}$, used to start our simulations was calculated from the stable stage distribution obtained from the arithmetic mean of the total number of flowering plants recorded in the population (exhaustive survey, Appendix A2) from 2010 to 2016, and the scaled eigenvector W from the arithmetic mean matrix over years (2010-2016) when pooling data over populations (see text for details). Extinction probability at a given time t corresponds to the number of trajectories for which $N(t) < 1$ over the total number of trajectories. $T_{0.5}$ represents the time corresponding to an extinction probability equal to $P = 0.5$.
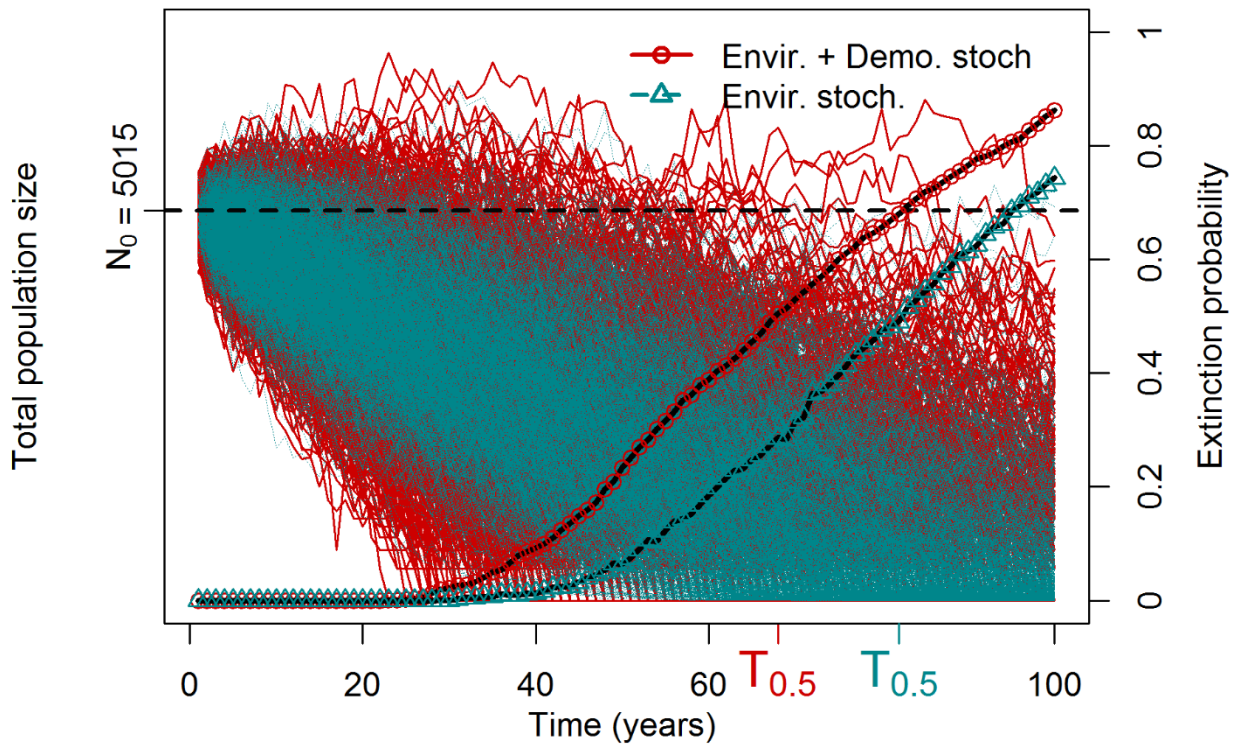
Appendix G: Required values of lower-level vital rates for achieving population persistence in a deterministic model ($\lambda_a = 1$), using two different methods: lower-level vital rates values were either predicted from the elasticity values, or directly from the global mean matrix after pooling individuals over populations and years to obtain a single population. For both methods, we varied only one vital rate at a time, while keeping others at their observed value in the mean matrix.

Vital rates	Observed value	Required value	
		Elasticity prediction	Prediction from the global matrix
Survival of just-emerged seedling s_0	0.477	0.811	0.790
Rosette survival s_2	0.707	0.918	0.937
Fecundity term f	11.16	18.98	18.50